Antitumor Activity of the Novel Oral Heat Shock Protein 90 Inhibitor in Mono Therapy and Combination Therapy

January 2020

Naomi ONO

Antitumor Activity of the Novel Oral Heat Shock Protein 90 Inhibitor in Mono Therapy and Combination Therapy

A Dissertation Submitted to
the Graduate School of Life and Environmental Sciences,
the University of Tsukuba
in Partial Fulfillment of the Requirements
for the Degree of Doctor of Philosophy in Biological Science
(Doctor Program in Biological Sciences)

Naomi ONO

Table of contents

Contents **Pages**

Abstract

Heat shock protein 90 (HSP90) is a molecular chaperone that plays a significant role in the stability and maturation of client proteins, including oncogenic targets for cell transformation, proliferation, and survival. It is an attractive target for cancer therapy. Recently, a novel HSP90 inhibitor (CH5164840) was identified, and its induction of oncogenic client protein degradation, anti-proliferative activity, and apoptosis investigated using the NCI-N87 gastric and BT-474 breast cancer cell lines. Interestingly, CH5164840 demonstrated tumor selectivity both *in vitro* and *in vivo*, binding to tumor HSP90, which forms active super chaperone complexes, rather than the HSP90 of normal cell, which mainly exist as non-complexes with co-chaperons *in vitro*. It is extensively distributed in mouse model tumors. These facts support the CH5164840-induced phosphorylated AKT level decrease observed in tumor tissues, but not in normal tissues. In addition to being well tolerated, orally administered CH5164840 exerts potent antitumor efficacy, leading to regression in the NCI-N87 and BT-474 tumor xenograft models. Additionally, CH5164840 significantly enhanced antitumor efficacy against the gastric and breast cancer models when co-administered with the human epidermal growth factor receptor 2 (HER2)-targeted agents trastuzumab and lapatinib. These data demonstrate the potential antitumor efficacy of monotherapy with CH5164840, and the significant synergistic efficacy of its co-administration with trastuzumab or lapatinib, validifying clinical development of CH5164840 as an HSP90 inhibitor for combination therapy with HER2-targeted agents against HER2-overexpressing tumors.

Epidermal growth factor receptor (EGFR) is one of the most potent oncogenic client proteins of HSP90. Targeted inhibition of EGFR has shown clinical efficacy in the treatment non-small-cell lung cancer (NSCLC) patients. However, primary and acquired resistance to existing EGFR inhibitors is a major clinical problem. In the present study, the antitumor activity of a combination of erlotinib and CH5164840 was investigated. The NSCLC cell lines and xenograft models were treated with CH5164840 and erlotinib to examine their mechanisms of action and cell growth inhibition. CH5164840 showed remarkable antitumor activity against the NSCLC cell lines and xenograft models. Combination therapy with CH5164840 enhanced the antitumor activity of erlotinib against NCI-H292 EGFR-overexpressing xenograft models. In vitro treatment of NCI-H292 cells with erlotinib resulted in increased STAT3 phosphorylation. Next, the role of the STAT3 signal in the mechanism of action of the erlotinib and CH5164840 combination was evaluated, as it is an important tumor growth-related signal. STAT3 phosphorylation increase in erlotinib-treated NCI-H292 cells was abrogated by HSP90 inhibition. Additionally, CH5164840 enhanced the antitumor activity of erlotinib, despite the low efficacy of erlotinib monotherapy, in a NCI-H1975 T790M mutation erlotinib-resistant model. Further, extracellular signal-regulated kinase (ERK) signaling was effectively suppressed by the erlotinib and CH5164840 co-therapy, in a NCI-H1975 erlotinib resistant model. These data collectively indicate the potent antitumor activity of CH5164840 and higher efficacy of its coadministration with erlotinib

against NSCLC tumors with EGFR overexpression and mutations. Therefore, providing evidence of the therapeutic potential of CH5164840 as an HSP90 inhibitor for combination therapy with EGFR-targeting agents against EGFR-addicted NSCLC.

Abbreviations

17-AAG	17-N-allylamino-17-demethoxygeldanamycin
17-DMAG	17-dimethylaminoethylamino-17-demethoxygeldanamycin
ABCG2	ATP binding cassette subfamily G member 2
Ab	antibody
AC	adenocarcinoma
ALK	anaplastic lymphoma kinase
c-PARP	cleaved poly (ADP-ribose) polymerase
EGFR	epidermal growth factor receptor
ER	estrogen-receptor
ERK	extracellular signal-regulated kinase
GAPDH	glyceraldehyde-3-phosphate dehydrogenase
HER2	human epidermal growth factor receptor 2
HER3	human epidermal growth factor receptor 3
HER4	human epidermal growth factor receptor 4
HSP90	heat shock protein 90
IP	immunoprecipitation
JAK	Janus kinase
Kd	dissociation constant
MDR	multidrug-efflux transporter
MTD	maximum tolerated dose
NQO1	NAD(P)H quinone dehydrogenase 1
NSCLC	non-small-cell lung cancer
p.o.	per os
PARP	poly-(ADP-ribose) polymerase
PBMC	peripheral blood mononuclear cells
PR	progesterone-receptor
PTEN	phosphatase and tensin homolog
q.d.	quaque die
SC	squamous cell carcinoma
SCLC	small cell lung cancer
STAT3	signal transducer and activator of transcription 3
TGI	tumor growth inhibition
TKI	tyrosine kinase inhibitor
TYK2	tyrosine kinase 2
TV	tumor volume

General introduction

Heat shock protein 90 (HSP90) is a highly conserved and ubiquitously expressed molecular chaperone in eukaryotic and prokaryotic cells, which plays key roles in protein folding and client protein stability (1). Oncogenic client proteins, the targets of many anticancer agents, encompass dysregulated, mutated, and fusion proteins, and are particularly dependent on HSP90 for conformation maintenance (2-6). For example, epidermal growth factor receptor (EGFR) is one of the most potent oncogenic client proteins of HSP90. Additionally, mutated EGFR seems to be more sensitive than wild-type EGFR to HSP90 inhibitor degradation (7, 8). HSP90 function inhibition is known to simultaneously lead to the degradation of multiple client proteins involved in tumor progression and inhibition of multiple oncogenic pathways, resulting in signal transduction loss, growth inhibition, cell death, and antiangiogenesis. Moreover, in tumor cells, HSP90 is present in an activated super-chaperone complex (9), and elevated HSP90 expression is associated with poor prognosis in breast cancer patients (10). Therefore, HSP90 targeting is considered a promising anticancer therapy strategy (11-14).

HER family members are one of the most potent oncogenic client proteins of HSP90. The HER family has four known members: human epidermal growth factor receptor 1 (HER1) (also termed EGFR), human epidermal growth factor receptor 2 (HER2), human epidermal growth factor receptor 3 (HER3), and human epidermal growth factor receptor 4 (HER4). They are structurally related receptor tyrosine kinases, which form homo- or hetero-dimer complexes with each other to contribute to the growth signal; the HER2 and HER3 heterodimer complex has a strong transforming activity. Aberrant signaling through the HER pathway is found in many epithelial cancer types (15).

Among females, breast cancer is the most commonly diagnosed cancer and leads to the highest number of cancer-related deaths worldwide (16). Breast cancer comprises a heterogeneous group of diseases in term of differentiation, proliferation, prognosis, and treatment. Several breast cancer molecular subtypes have been identified, based on hormone receptor (estrogen-receptor (ER), progesterone-receptor (PR)) and HER2 status (17). One of these subtypes is the HER2-enriched subtype, which occurs in 15–20% of breast cancer patients. The overexpression of HER2, a receptor tyrosine kinase and oncogene, is associated with poor prognosis in breast (18) and gastric (19) cancers. The HER2 receptors are anticancer drug targets. Two strategies for blocking the action of these proteins include ectodomain targeting with antibodies (Ab) and the use of protein-tyrosine kinase activity-inhibiting drugs. Although trastuzumab, (humanized monoclonal Ab directed against HER2) and lapatinib (EGFR and HER2 dual-kinase inhibitor) have both demonstrated good initial clinical responses and are considered standard-of-care agents, clinical relapse with trastuzumab or lapatinib therapy has been observed in some patients (20). Therefore, more effective HER2-overexpressing tumor treatments are required, and the development of rationalized combinations of agents appears particularly promising (21).

Lung cancer is one of the most commonly diagnosed cancer and cause of cancer-related deaths worldwide (16), including the US (22). It is classified into two main types: small cell lung cancer (SCLC) and non-SCLC (NSCLC), which account for approximately 85% of all lung cancers (23, 24). Furthermore, NSCLCs are characterized into two major subtypes: adenocarcinoma (AC) and squamous cell carcinoma (SCC). The classification of NSCLC subtypes based on genotype and histology has resulted in dramatic improvements in disease outcome in selected patient. Specifically, molecular targeted drugs such as EGFR or Anaplastic lymphoma kinase (ALK) inhibitors, are approved for the treatment of NSCLC harboring genetic mutations in the genes encoding these proteins (25). Tumors with the EGFR gene that harbors activating mutations in exon 19 and 21, can be successfully treated with EGFR-tyrosine kinase inhibitors (TKIs), compared with cytotoxic agents (26, 27). Despite remarkable responses in patients with activating mutations in the tyrosine kinase domain of EGFR, most patients relapse within their first year of treatment. Due to the potential for resistance to TKI in EGFR-addicted tumors, identification of an effective treatment using rationalized agent combinations is particularly promising.

In recent years, promising molecular targeted drugs have been developed for cancer treatment, but drug resistance and recurrence remain clinical problems. With respect to blocking cancer-causing resistance mechanisms, unique features of HSP90 inhibition are expected to aid the overcoming of TKI resistance. First-generation HSP90 inhibitors: geldanamycin derivatives, are associated with hepatotoxicity, polymorphic metabolism by NAD(P)H quinone dehydrogenase 1 (NQO1), and efflux via P-glycoprotein, and are therefore not desirable for clinical use. Thus, they have not yet been approved for cancer therapy. To overcome these drawbacks, several second-generation HSP90 inhibitors have been synthesized and are currently in clinical development (28-31).

Recently, a novel potent HSP90 inhibitor CH5164840, with a unique chemical structure, based on a 3-D structure, was identified via virtual screening. In co-crystal structural analysis, CH5164840 was found to interact with an ATP-binding pocket of HSP90α with high affinity (32, 33). In the present study, to examine useful cancer treatment strategies using HSP90 inhibitors, the focus was placed on a HER2 positive cancer and NSCLC. In Chapter 1, the *in vitro* and *in vivo* investigations of the efficacy of a CH5164840 and HER2-targeted agent combination is examined. Additionally, the *in vitro* and *in vivo* properties of CH5164840 monotherapy and CH5164840 and erlotinib co-therapy, including its antitumor activity in EGFR overexpressing and erlotinib-resistant NSCLC xenograft models, are elucidated in Chapter 2.

Chapter 1

Preclinical antitumor activity of the novel heat shock protein 90 inhibitor CH5164840, against human epidermal growth factor receptor 2 (HER2)-overexpressing cancers

1. Introduction

The HER family is composed of four HER receptors: HER1 (also termed EGFR), HER2, HER3, and HER4 (15). HER family members can form homodimers and heterodimers with each other. No known ligand binds HER2 with high affinity. HER2 forms heterodimers with each of the other family members, and these heterodimers can bind to growth factors (34). Although HER3 has a tyrosine kinase domain that is highly homologous to other family members, its kinase activity is impaired. HER3 can also form heterodimers with the other family members. However, owing to the lack of protein kinase activity by HER3, transphosphorylation by other HER family members is required for cell signaling. It is known that the HER2 and HER3 heterodimer complex has a strong transforming activity.

The overexpression of HER2, an oncogenic receptor tyrosine kinase, is associated with poor prognosis in breast (18) and gastric (19) cancers. Indeed, in HER2-overexpressing breast cancers, HER2 and HER3 frequently form a heterodimer as an oncogenic unit that plays an important role in HER2-mediated signaling (7, 8, 35). Although both trastuzumab and lapatinib are considered standard-of-care agents and benefit HER2-amplified breast and gastric cancer patients, clinical relapse with both has been observed in some patients (20). Therefore, more effective treatment of HER2-overexpressing tumors is required, and forming rationalized agent combinations appears particularly promising (21).

As HER2 is a representative client protein whose stability is HSP90-function dependent (36-38), HSP90 inhibitors are effective against HER2-overexpressing tumors (39, 40). HSP90 is an attractive target of cancer therapies. Geldanamycin and its derivatives 17-AAG, 17-DMAG, and first generation HSP90 inhibitors, show strong efficacy *in vivo*. However, these inhibitors are reportedly oxidized by NQO1 and effluxed by multidrug-efflux transporter (MDR) and ATP binding cassette subfamily G member 2 (ABCG2, also termed BCRP); thus, attenuating their efficacy. Additionally, they are hepatotoxic. Recently, a novel HSP90 inhibitor: CH5164840, was generated (32, 33). To examine the usefulness of its significant antitumor efficacy in HER2 positive tumors, *in vitro* and *in vivo* investigations of the efficacy of CH5164840 and HER2-targeted agent combination, were performed.

2. Materials and Methods

2- 1. Compound

CH5164840 (33), its biotin-labeled version, and 17-dimethylaminoethylamino-17-demethoxygeldanamycin (17-DMAG) were synthesized by Chugai Pharmaceutical (Kanagawa, Japan). Lapatinib was prepared from the commercial product Tykerb (GlaxoSmithKline, Clifton, NJ, USA). Trastuzumab was obtained from Chugai Pharmaceutical／F. Hoffmann-La Roche (Basel, Switzerland).

2- 2. Cells and culture

The human gastric cell line NCI-N87; breast cancer cell lines BT-474, SK-BR-3, and MDA-MB-231; ovarian cancer cell line SK-OV-3; prostate cancer cell line DU 145; colorectal cancer cell line HCT116; and NSCLC cell line NCI-H460 were obtained from the American Type Culture Collection (ATCC; Manassas, VA, USA). The human gastric cell line JR-St, was obtained from Immuno-Biological Laboratories (Fujioka, Japan). Adult normal human dermal (NHDF-Ad) fibroblast cells were obtained from Takara Bio (Shiga, Japan). Human mammary tumor MAXF401 was obtained from Professor Heinz-Herbert Fiebig (University of Freiburg, Freiburg, Germany). All cell lines were cultured according to the supplier's instructions.

2- 3. Cell proliferation assay

Tumor cells were seeded into microtiter plates containing compounds and incubated at 37°C in 5% CO_2. After a 4-day incubation, Cell Counting Kit-8 solution (Dojindo Laboratories, Kumamoto, Japan) was added, and absorbance at 450 nm measured with the Microplate-Reader iMark (Bio-Rad Laboratories, Hercules, CA, USA). Anti-proliferative activity was calculated using the formula: $(1-T/C) \times 100$ (%), where T represents the absorbance of drug-treated cells, and C represents that of untreated control cells at 450 nm. The IC_{50} values were calculated using Microsoft Excel 2007 (Redmond, WA, USA).

2- 4. Surface plasmon resonance analysis

All biosensor experiments were conducted using a Biacore 2000 instrument (GE Healthcare Japan, Tokyo, Japan). The N-terminal domains of the human HSP90α (9–236) and HSP90β (1–221) expressed in *Escherichia coli* were minimally biotinylated (sulfo-NHS-LC-LC biotin; Thermo Fisher Scientific, Waltham, MA, USA) and coupled on a streptavidin-coated sensor chip (GE Healthcare, Buckinghamshire, UK), respectively. Sensorgrams were processed using SCRUBBER2 (BioLogics, Campbell, Australia) and *Kd* values were determined by fitting the processed data globally to the 1:1 binding model, using BIAevaluation (version 3.1; GE Healthcare). The experiments for the *Kd* determinations were performed in 50 mM

tris(hydroxymethyl)aminomethane-HCl (pH 7.6), 150 mM NaCl, 0.005% P-20, and 1% DMSO at 30 μL/min, 20°C.

2- 5. Protein kinase assay

The activities of EGFR, KIT, HER2, MET, fibroblast growth factor receptor 2 (FGFR2), FMS-related tyrosine kinase 3 (FLT3), leukocyte receptor tyrosine kinase (LTK), insulin receptor (INSR), YES, ABL, ZAP70, insulin-like growth factor receptor I (IGF1R), vascular endothelial growth factor receptor 2 (KDR) (Life Technologies), and platelet derived growth factor receptor (PDGFR)β (Millipore) on substrate peptides were determined using a homogeneous time-resolved fluorescence assay with LANCE Eu-W1024 labeled anti-phosphotyrosine PT66 antibody (PerkinElmer), according to standard methods. Time-resolved fluorescence was measured with an EnVision HTS microplate reader. The activities of Aurora A, AKT1/PKBα, PKA, CDK1/cyclin B, CDK2/cyclin A (Millipore), PKCα, PKCβ1, PKCβ2, ALK, and JAK1 (Carna Biosciences) on substrate peptides were determined using the IMAP FP Screening Express Progressive Binding System (Molecular Devices). Specifically, to detect MEK activity, inactive MAP kinase 2/ERK2 (Millipore) was activated by MAP2K1 (Carna Biosciences) addition; then, MAP kinase 2 activity on a substrate peptide was determined using the IMAP FP Screening Express Progressive Binding System. Fluorescence polarization was measured with an EnVision HTS microplate reader. p70S6K activity on a substrate peptide was determined using the Z'-LYTE Kinase Assay Kit-Ser/Thr 7 Peptide (Life Technologies). Time-resolved fluorescence was measured with an EnVision HTS microplate reader.

2- 6. Western blotting and co-immunoprecipitation

Cells were lysed with Cell Lysis Buffer (Cell Signaling Technology) containing protease and phosphatase inhibitors. Before lysis, the grafted tumors were homogenized using a BioMasher (K.K. Ashisuto). The lysates were denatured with Sample Buffer Solution with Reducing Reagent for SDS-PAGE (Nacalai Tesque), and then subjected to SDS-PAGE. After electroblotting, the polyvinylidene fluoride membranes were blocked with Blocking One (Nacalai Tesque) for 1 hour. Membranes were then incubated with primary antibodies (see below) at room temperature for 2 hours or at 4°C overnight, followed by washing three times with 0.1% Tween 20 (Nacalai Tesque) in TBS buffer (TBS-T buffer; TaKaRa Bio). This was followed by a 1-hour incubation at room temperature with secondary antibodies (Cell Signaling Technology). Then, membranes were washed with TBS-T buffer, followed by incubation with ECL or ECL-plus solutions (GE Healthcare). Signals were detected with ECL Plus (GE Healthcare), followed by LAS-4000 (Fujifilm, Tokyo, Japan) or the Odyssey Infrared Imaging System (LI-COR Biosciences, Lincoln, NE, USA). The primary antibodies used were used were pY1221-HER2, pY1068-EGFR, pY1289-HER3, pS473-AKT, AKT, pT202/Y204-ERK, ERK (Cell Signaling, Beverly, MA, USA), EGFR, HER2, HER3, and actin (Santa Cruz Biotechnology,

Santa Cruz, CA, USA), and HSP70 (Stressgen, Victoria, Canada). For co-immunoprecipitation, cell lysates were incubated with or without the HSP90 antibody (Santa Cruz Biotechnology) overnight at 4°C, and protein A-agarose beads (Roche Diagnostics, Penzberg, Germany) added for 1 h at 4°C. Beads were then washed three times with cell lysis buffer, boiled with sample buffer solution, and analyzed via Western blotting.

2- 7. Xenograft model and efficacy study

All animal studies were approved by the Chugai Institutional Animal Care and Use Committee. Cancer cells (0.5–1 × 107) were implanted subcutaneously into the right flank of athymic nude (BALB/c nu/nu) mice (CAnN.Cg-Foxn1<nu>/CrlCrlj nu/nu; Charles River Laboratories, Kanagawa, Japan). Tumor volume (TV) was calculated using the formula: $TV = ab^2/2$, where a and b represent tumor length and width, respectively. Once the tumors had reached a volume of approximately 200–300 mm^3, the animals were randomized into each group (n = 4 or 5), and treatment was initiated. CH5164840 and lapatinib were orally administered; trastuzumab was administered by intraperitoneal injection. Tumor growth inhibition (TGI) was calculated using the formula: $TGI = (1-[T_t-T_0]/[C_t-C_0]) \times 100$ (%), where T (TV of treated group; T_0 on day 0 or T_t on day t) and C (TV of control group; C_0 on day 0 or C_t on day t) represent mean tumor volume. The maximum tolerated dose (MTD) was defined as the dose that resulted in neither lethality nor more than 20% body weight loss. The ED_{50} was calculated from the values of TGI on the final experimental day using XLfit version 5.1.0.0 (Microsoft, Redmond, WA, USA).

2- 8. Pharmacokinetic and pharmacodynamic study

Tumor xenograft (NCI-N87)-bearing nude mice were prepared by the same method used for the efficacy studies. Two mice were killed after oral administration of 50 mg/kg CH5164840, for collection of the indicated organs and grafted tumors. CH5164840 was extracted with acetonitrile/water/formic acid (75/25/0.1, v/v/v) under ice-cold conditions. CH5164840 concentration was determined using liquid chromatography/tandem mass spectrometry (LC/MS/MS) (API 3000, Applied Biosystems, Foster City, CA, USA).

2- 9. Real-time quantitative RT-PCR

The QuantiTect Probe RT-PCR kit (Qiagen, Valencia, CA, USA) and Taqman primers (Applied Biosystems) were used to perform all reactions. Total RNA extraction was performed with the RNeasy mini kit (Qiagen). For the data analysis, counts were normalized to a housekeeping gene (Glyceraldehyde-3-phosphate dehydrogenase, GAPDH) at the same time point and condition. Counts are reported as fold change relative to the untreated control.

2- 10. Statistical analysis

SAS preclinical package software (version 5; SAS, Cary, NC, USA) was used for the statistical analyses (Tukey's test). Statistically significant differences are indicated with asterisks; $^{**}P < 0.01$ and $^{***}P < 0.001$.

3. Results

3- 1. CH5164840, a novel HSP90 inhibitor, induces the degradation of multiple HSP90 client proteins and apoptosis in NCI-N87 and BT-474 HER2-overexpressing cells.

Recently, CH5164840 was identified as an HSP90 inhibitor with a novel chemical structure, through virtual screening based on a 3-D structure (32, 33). As shown in Fig. 1-1, the binding affinity of CH5164840 for HSP90α was found to be 0.52 and 1.4 nM for HSP90β, a level that is associated with a slow dissociation rate. Specificity to the ATP-binding pocket of HSP90 was indicated by no inhibition against 22 kinases (IC_{50} > 20 μM) in a cell-free kinase assay and the absence of significant ATP competitive binding (DiscoveRx, Fremont, CA, USA) against 400 kinases at 10 μM. Firstly, the sensitivity of various cancer cell lines to CH5164840 with *in vitro* cell growth assays was evaluated. The IC_{50} values of CH5164840 were found to be 66–260 nM in nine cancer cell lines (Table 1-1). CH5164840 also showed *in vitro* sensitivity against 17-DMAG-resistant cell lines, NCI-H460-PTX250, which overexpress MDR1 and MDA-MB-231 with NQO1 C609T mutation (Table 1-3). Secondly, CH5164840-induced client protein degradation in cancer cells was examined. CH5164840 was found to significantly reduce phosphorylation and protein levels of HER2, HER3, and EGFR, and inhibit downstream signals in NCI-N87 (HER2-overexpressing gastric cancer) and BT-474 (HER2-overexpressing breast cancer) cells. Furthermore, activated caspase-3/7 levels (Figs. 1-2b, d) and cleaved poly (ADP-ribose) polymerase (Figs. 1-2a, c) increased following exposure to CH5164840, indicating that CH5164840 induces apoptosis. HSP70 induction was examined as it is a known response marker of HSP90 inhibition. The results confirmed that like 17-DMAG, HSP70 expression were induced by CH5164840 *in vitro* (Figs. 1-2a, c). In a time-course study, CH5164840 and 17-DMAG caused client protein degradation and HSP70 induction (Fig. 1-2e). These results indicate that CH5164840 selectively inhibited HSP90, induced key client protein degradation, and suppressed both the PI3K/AKT survival and RAF/MEK/ERK signaling pathways, leading to apoptosis induction and inhibition of tumor proliferation.

3- 2. CH5164840 exhibits tumor-selective HSP90 inhibition.

Based on the observation of tumor HSP90 in super-chaperone complexes with high ATPase activity and its high binding affinity to the HSP90 inhibitor 17-allylamino-17-demethoxy-

geldanamycin (17-AAG) (7), the tumor selectivity of CH5164840 was assessed using the following procedure. Firstly, the anti-proliferative activity of CH5164840 in normal fibroblast (NHDF-Ad) cells was compared to that in NCI-N87 tumor cells, revealing that NHDF-Ad cell proliferation was moderately inhibited by CH5164840 treatment (IC_{50}, 1.2 μM), and that the cells were less sensitive to CH5164840 than NCI-N87 and other cancer cells (Table 1-1; Fig. 1-3a). Next, to examine whether CH5164840 binds selectively to tumor HSP90, pull-down assays were conducted with a biotin-labeled CH5164840 (Bio-CH) probe using cell extracts prepared from NCI-N87 or NHDF-Ad cell lines. As shown in Fig. 1-3b, Bio-CH preferentially bound to HSP90 when it formed a super-chaperone complex with the co-chaperones HSP70, HOP, and HSP40, in NCI-N87 cells, rather than to HSP90 in NHDF-Ad cells, which remained mainly free from these co-chaperones. These data indicate that CH5164840 selectively binds to tumor HSP90, which forms a super-chaperone complex. Further, tumor-selective distribution of CH5164840 after a single administration in mice, was explored. CH5164840 was only detected in tumor samples 48h after oral administration of one dose of 50 mg/kg CH5164840 in the NCI-N87 xenograft model. Greater CH5164840 retention was observed in tumor tissues (half-life = 6.3 h) compared to normal tissues and plasma (Fig. 1-3c). Finally, AKT phosphorylation level in tumor and normal tissue was measured to determine CH5164840 associated to tumor-selective HSP90 inhibition *in vivo* in NCI-N87 models. The results indicate that CH5164840 reduces AKT phosphorylation in tumor tissues, but not in normal tissue (Fig. 1-3d). Additionally, HSP70 induction in tumor and normal tissue was confirmed. Collectively, these results indicate that preferential binding to tumor HSP90 and increased retention in tumors lead to tumor-selective HSP90 inhibition by CH5164840.

3- 3. CH5164840 demonstrates potent antitumor efficacy in xenograft models.

The *in vivo* antitumor efficacy of CH5164840 against human tumor xenograft models in mice, was investigated. Daily oral administration of CH5164840 resulted in significant dose-dependent antitumor efficacy in the NCI-N87 and BT-474 xenograft models, with a maximum TGI of 160% and 152%, respectively (Figs. 1-4a, b), without any significant loss of body weight. Additionally, HER2, HER3, EGFR, cyclinD1, and phospho-AKT protein levels significantly decreased in the NCI-N87 xenograft model, resulting in CH5164840 inhibition of downstream signals (Fig. 1-4c). Further, CH5164840 demonstrated significant antitumor efficacy against various xenograft models (Table 1-2). These results are consistent with those regarding the *in vitro* antitumor activity and tumor-selective HSP90 inhibition of CH5164840.

3- 4. CH5164840 enhances the antitumor efficacy of HER2-targeted therapy with trastuzumab or lapatinib.

The combined effect of CH5164840 and a HER2-targeted therapy, was examined. Administration

of a combination of 25 mg/kg CH5164840 and 30 mg/kg trastuzumab to the trastuzumab-sensitive NCI-N87 and BT-474 xenograft models resulted in the enhancement of the antitumor efficacy of trastuzumab by CH5164840, increasing its TGI as a single agent from 56% to 167% in the NCI-N87 model (Fig. 1-5a), and from 136% to 240% in the BT-474 xenograft model (Fig. 1-5b). With regards to lapatinib, co-administration of 100 mg/kg lapatinib and 12.5 mg/kg CH5164840 to the NCI-N87 and BT-474 xenograft models resulted in significant enhancement of the antitumor efficacy of lapatinib by CH5164840 in both the NCI-N87 (TGI = 45% lapatinib only vs 155% in combination; Fig. 1-5c) and BT-474 xenograft (TGI = 88% lapatinib only vs 214% in combination; Fig. 1-5d) model. In all cases, the co-therapy-enhanced efficacy was statistically significant. These results suggest that CH5164840 potentiates the efficacy of HER2-targeted agents.

Furthermore, when the efficacy of intermittent dosing was examined in the form of once- or twice-weekly regimens of 50 mg/kg CH5164840 in the NCI-N87 xenograft model, CH5164840 was found to enhance the antitumor efficacy of trastuzumab (TGI = 69% with trastuzumab only vs 97% or 123% with combined trastuzumab and once- or twice-weekly CH5164840 administration, respectively; Fig. 1-7).

3- 5. CH5164840 suppresses lapatinib treatment-induced HER3 signal activation *in vitro*.

The mechanism underlying the synergistic efficacy of the combination of CH5164840 and lapatinib was examined, owing to elucidation of this synergism. Firstly, HER3 expression was examined after lapatinib treatment in NCI-N87 cells, as lapatinib treatment reportedly induces HER3 expression in SK-BR-3 cells (41). Quantitative RT-PCR revealed that lapatinib induced HER3 mRNA expression (Fig. 1-6a). HER3 protein levels consistently increased in a time-dependent manner (Fig. 1-6b). Although HER3 phosphorylation was transiently inhibited by lapatinib, it was not long lasting, despite continuous lapatinib treatment (Fig. 1-6b). Additionally, lapatinib discontinuation after 24 h of treatment, followed by lapatinib-free incubation, resulted in hyper-phosphorylation of HER3 (Fig. 1-6c). Next, to determine whether HSP90 inhibition induced the degradation of lapatinib-induced HER3 and other clients, the effect of CH5164840 was investigated in NCI-N87 cells. As shown in Fig. 1-6d, HER2 and EGFR were degraded, and their phosphorylation and downstream signals significantly decreased by CH5164840 and lapatinib co-therapy. Interestingly, lapatinib-induced HER3 returned to basal levels after the addition of CH5164840. Finally, HER3 was observed to be strongly co-precipitated with HSP90 in lapatinib-treated cells compared to that in non-treated control cells, and importantly, was returned to basal levels by the addition of CH5164840 (Fig. 1-6e).

4. Discussion

First-generation HSP90 inhibitors: geldanamycin derivatives, are associated with hepatotoxicity,

polymorphic metabolism by NQO1, and efflux by P-glycoprotein. They are therefore undesirable for therapeutic use and have not yet been approved for cancer therapy. To overcome these drawbacks, a novel HSP90 inhibitor CH5164840, with a unique chemical structure, was generated through virtual screening based on a 3-D structure. Its *in vitro* sensitivity against the 17-DMAG-resistant cell lines NCI-H460-PTX250, which overexpress MDR1 and MDA-MB-231, which have NQO1 C609T mutation, was confirmed. An attractive feature of HSP90 as an antitumor target is the possibility of tumor selectivity. As shown in Fig. 1-3b, a higher binding affinity of bio-CH to tumor HSP90 compared to normal HSP90, was observed. In this pull-down assay, the biotin label was positioned based on the co-crystal structure of HSP90α with CH5164840, to prevent influence on CH5164840–HSP90 binding. This selective binding of CH5164840 to HSP90 in tumor tissues and its long retention in tumor tissues in the mouse model explain why tumor tissue phosphorylated AKT levels, but not that of normal tissues, were observed to be lower in the pharmacodynamics study, indicating the tumor-selectivity of HSP90 inhibition by CH5164840.

Furthermore, CH5164840 enhanced the antitumor efficacy of the HER2-targeted therapies trastuzumab and lapatinib, in the NCIN87 and BT-474 tumor models. In combination with trastuzumab in the NCI-N87 xenograft model, antitumor efficacy was sustained over the follow-up period without any additional administration. Furthermore, in the form of once- or twice-weekly regimens of 50 mg/kg CH5164840 in the NCI-N87 xenograft model, CH5164840 was found to enhance the antitumor efficacy of trastuzumab. In other words, variety schedule regimen of CH5164840 is possible in combination therapy. The efficacy of the combination of CH5164840 and trastuzumab observed in the present study is similar to the findings of a preclinical study (39) and a phase I study in which a combination of 17-AAG and trastuzumab was well tolerated and demonstrated clinical efficacy in HER2-overexpressing breast cancer patients whose tumors had progressed during trastuzumab treatment (40). Additionally, as shown in Figs. 1-5(c, d), when a reduced-dosage regimen was evaluated by combining 12.5 mg/kg CH5164840 (one-quarter of the MTD dose for single-agent administration) with lapatinib, the reduced dosage of CH5164840 still enhanced the antitumor efficacy of lapatinib. These results suggest that CH5164840 administration at reduced frequencies and doses, which might aid the avoidance of possible side-effects, still provides a high level of antitumor efficacy in combination with HER2-targeted agents.

As shown in Fig. 1-6, the molecular mechanisms behind CH5164840-induced enhancement of the antitumor efficacy of agents was examined by elucidating HER3 induction by lapatinib in the NCI-N87 cells, as previously reported in SK-BR-3 cells (41). Lapatinib therapy cessation as found to lead to HER3 hyper-phosphorylation during a previous study regarding gefitinib-induced p-HER3 (42). These data suggest that lapatinib-induced HER3 confers resistance to lapatinib itself in NCI-N87 cells in a preclinical setting, and possibly in a clinical setting as well. Interestingly, this lapatinib- induced HER3 is strongly degraded by CH5184840, suggesting that lapatinib-induced HER3 is a preferred

client of HSP90, and is therefore sensitive to HSP90 inhibition. This hypothesis is strongly supported by the preferred binding of induced HER3 to HSP90 and its suppression by CH5164840. Overall, the results suggest that the HSP90 inhibitor CH5164840, could enhance the antitumor efficacy of lapatinib by effectively targeting lapatinib-induced HER3. This possibly unique feature of HSP90 inhibition is strongly supported by a recent report by Chandarlapaty et al. (43), who showed that an HSP90 inhibitor prevented the production of AKT inhibitor-induced receptor tyrosine kinases, resulting in a high efficacy. Conclusively, the characteristics of CH5164840, particularly its selective binding to tumor HSP90 and relatively long retention in tumor tissue, allow it to exert a potent antitumor activity, even when administered as a single agent. In this examination of the antitumor efficacy of CH5164840 both *in vitro* and *in vivo*, the combination of CH5164840 with HER2-targeted agents, especially lapatinib, was found to enhance the antitumor efficacy of the agent by degradation of lapatinib-induced HER3. These observations indicate that possibility of treating tumors whose growth and survival depend on HSP90 with a combination therapy of the HSP90 inhibitor CH5164840, and HER2-targeted therapies.

5. Tables

Table 1- 1. *In vitro* antitumor spectrum of CH5164840

Cancer cell lines	IC_{50} (μM)
NCI-N87 (Gastric cancer)	0.066
JR-St (Gastric cancer)	0.098
BT-474 (Breast cancer)	0.11
SK-BR-3 (Breast cancer)	0.067
MDA-MB231 (Breast cancer)	0.26
SK-OV-3 (Ovarian cancer)	0.26
DU145 (Prostate cancer)	0.15
NCI-H460 (NSCLC)	0.16
HCT116 (Colorectal cancer)	0.15

Table 1- 2. Spectrum of the antitumor efficacy of CH5164840 in various xenograft models

	Tumor growth inhibition (%)	ED_{50} (mg/kg)
NCI-N87 (Gastric cancer)	160	4.2
BT-474 (Breast cancer)	152	2.1
MDA-MB231 (Breast cancer)	80	7.1
MAXF-401 (Breast cancer)	97	11.0
SK-OV-3 (Ovarian cancer)	91	8.0
DU145 (Prostate cancer)	87	9.5
HCT116* (Colorectal cancer)	83	6.7

q.d.x11, p.o. at 50 mg/kg, * at 25 mg/kg

Table 1- 3. *In vitro* antitumor activity of CH5164840 vs 17-DMAG

	NCI-H460	**NCI-H460-PTX250** MDR overexpression	Ratio
	IC_{50} (μM)	IC_{50} (μM)	
CH5164840	0.25	1.9	7.6
17-DMAG	0.0020	2.2	1092
Docetaxel	0.0021	1.4	676

	KPL-4 NQO1 wt	**MDA-MB-231** NQO1 609T	Ratio
	IC_{50} (μM)	IC_{50} (μM)	
CH5164840	0.15	0.29	1.7
17-DMAG	0.0022	0.13	68

NQO1: NAD(P)H dehydrogenase, quinone 1

6. Figures

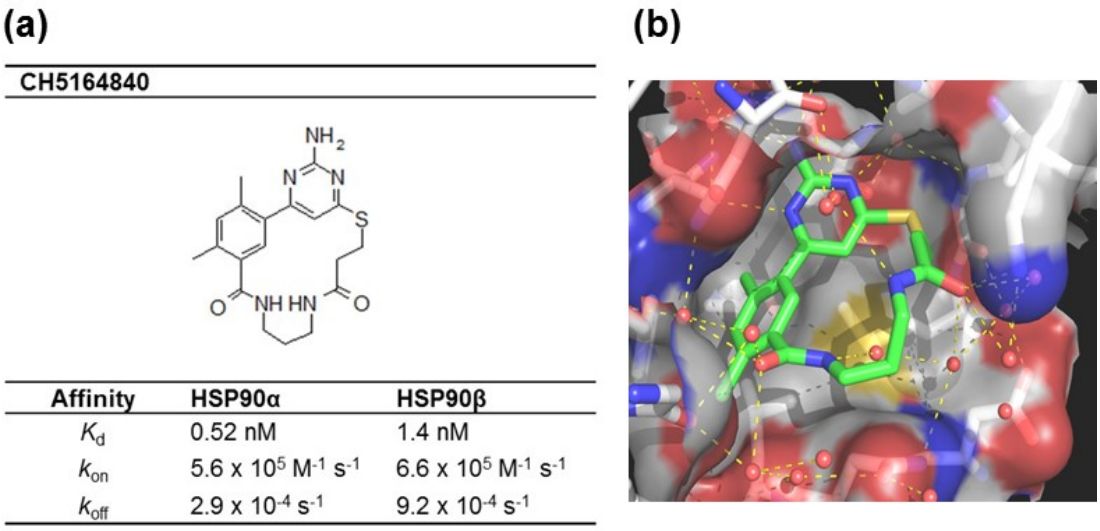

Fig. 1- 1 Chemical structure and binding affinity of CH5164840 to HSP90 protein.

(a) Chemical structure and binding affinity of CH5164840 to HSP90. (b) X-ray co-crystal structure of CH5164840 and HSP90α. (Modified finger. in ref. (33))

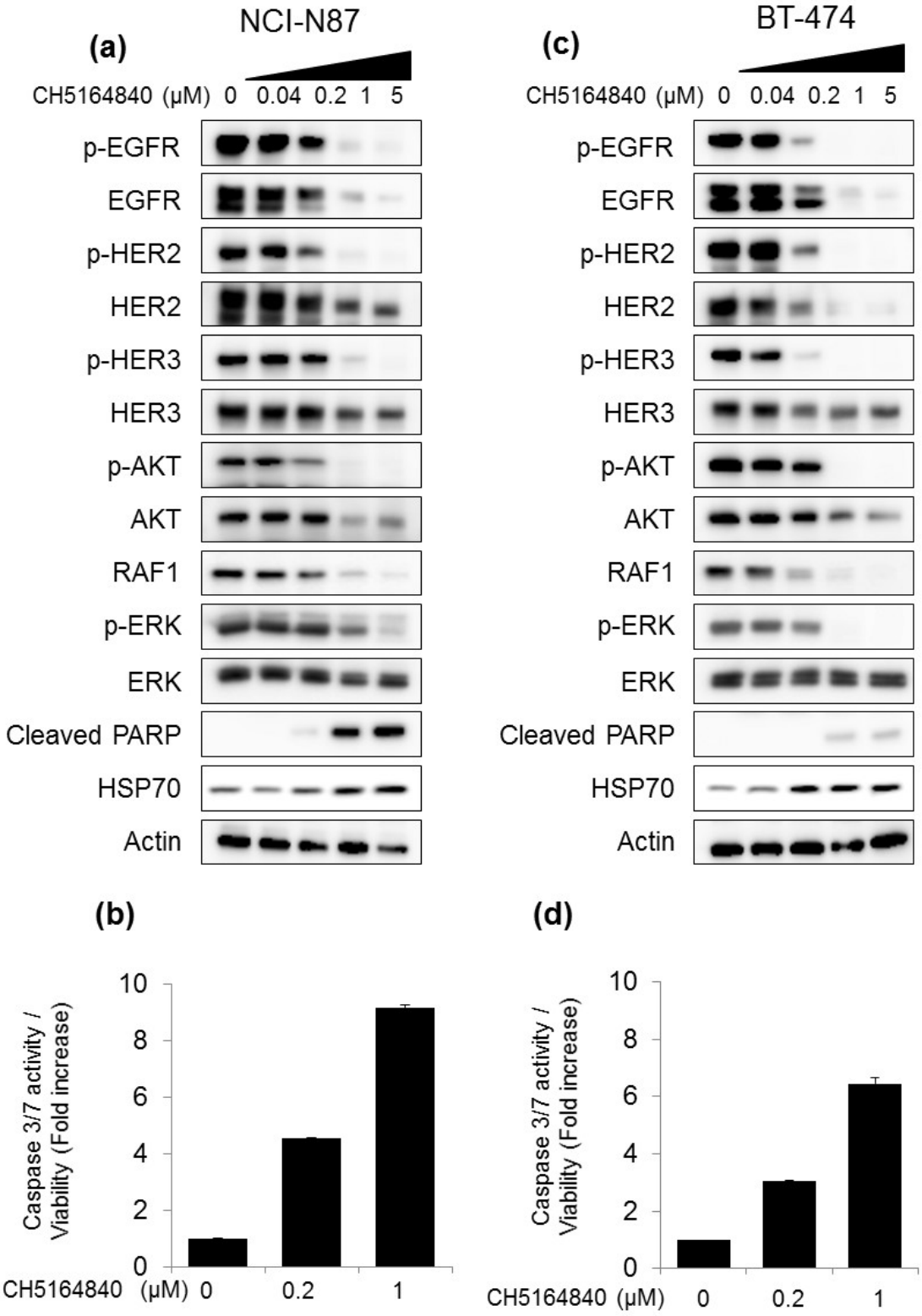
(a)
NCI-N87
CH5164840 (μM) 0 0.04 0.2 1 5
p-EGFR
EGFR
p-HER2
HER2
p-HER3
HER3
p-AKT
AKT
RAF1
p-ERK
ERK
Cleaved PARP
HSP70
Actin
(c)
BT-474
CH5164840 (μM) 0 0.04 0.2 1 5
p-EGFR
EGFR
p-HER2
HER2
p-HER3
HER3
p-AKT
AKT
RAF1
p-ERK
ERK
Cleaved PARP
HSP70
Actin
(b)
Caspase 3/7 activity / Viability (Fold increase)
10
8
6
4
2
0
CH5164840 (μM) 0 0.2 1
(d)
Caspase 3/7 activity / Viability (Fold increase)
10
8
6
4
2
0
CH5164840 (μM) 0 0.2 1

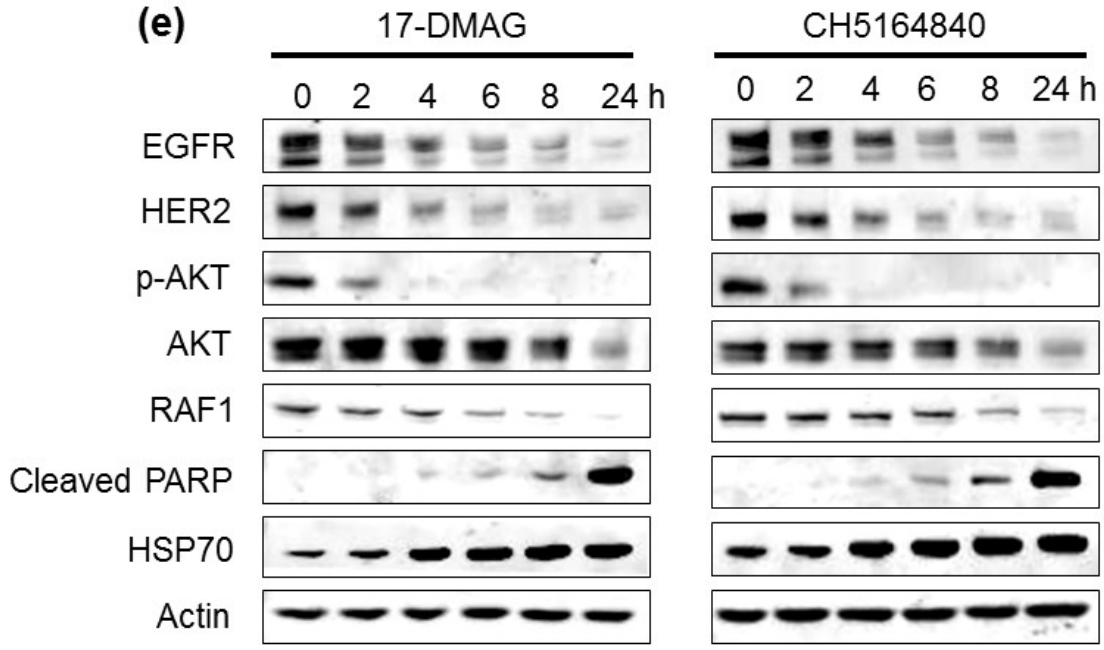

Fig. 1- 2. CH5164840 induces the degradation of multiple Hsp90 client proteins and apoptosis.

CH5164840 induces the degradation of multiple heat shock protein 90 (HSP90) client proteins and caspase-3/7-dependent apoptosis in HER2-positive cells. (a) (c) NCI-N87 or BT-474 cells were treated with the indicated concentrations of CH5164840 for 24 h before lysing and analysis using Western blotting. (b) (d) NCI-N87 and BT-474 cells were treated with 0, 0.2, or 1 μM of CH5164840 for 48 h. Caspase-3/7 activity and cell viability were measured with the CaspaseGlo3/7 assay and CellTiter-Gro, respectively, using EnVision High Throughput Screening. Caspase activity was normalized by cell viability. (e) NCI-N87 cells were treated with the 0.5 μM of 17-DMAG and 2 μM of CH5164840 for the indicated times before lysing and analysis using Western blotting. p-, phospho; PARP, poly (ADP-ribose) polymerase.

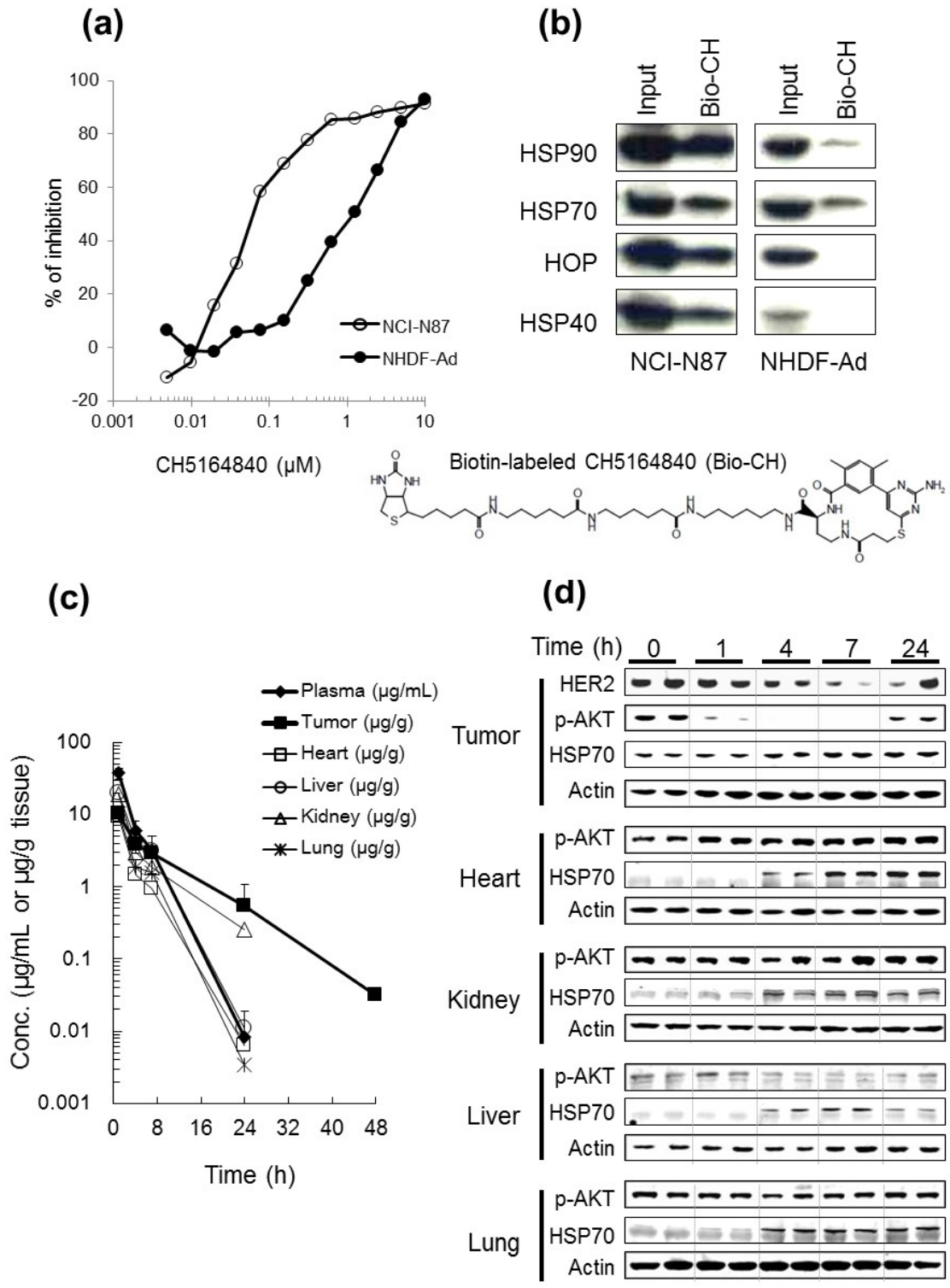

Fig. 1- 3. CH5164840 displays higher affinity to HSP90 with multi-chaperone complexes in tumor cells and tumor−selective retention of CH5164840 and pharmacodynamics.

(a) Normal fibroblast (adult normal human dermal [NHDF-Ad]) and tumor (NCI-N87) cell lines were incubated with different concentrations of CH5164840 for 4 days. Then, Cell Counting Kit-8 solution was added, and after incubation for several more hours, absorbance at 450 nm was measured with a microplate reader. The vertical axis shows the percentage of inhibition relative to the DMSO control. (b) NHDF-Ad and NCI-N87 cell lysates were precipitated with biotin-labeled CH5164840 (Bio-CH) and analyzed using Western blotting with the indicated antibodies. (c) Mice with established NCI-N87 xenografts were orally administered a single dose of 50 mg/kg CH5164840 and killed at the indicated times. Plasma and sample tissues were removed and homogenized, and the CH5164840 concentration of plasma, heart, kidney, liver, lung, and tumor analyzed using liquid chromatography/tandem mass spectrometry (LC/MS/MS). Data are shown as mean ± SD (n = 3). (d) Lysates were prepared from the tumor and organs and analyzed using Western blotting.

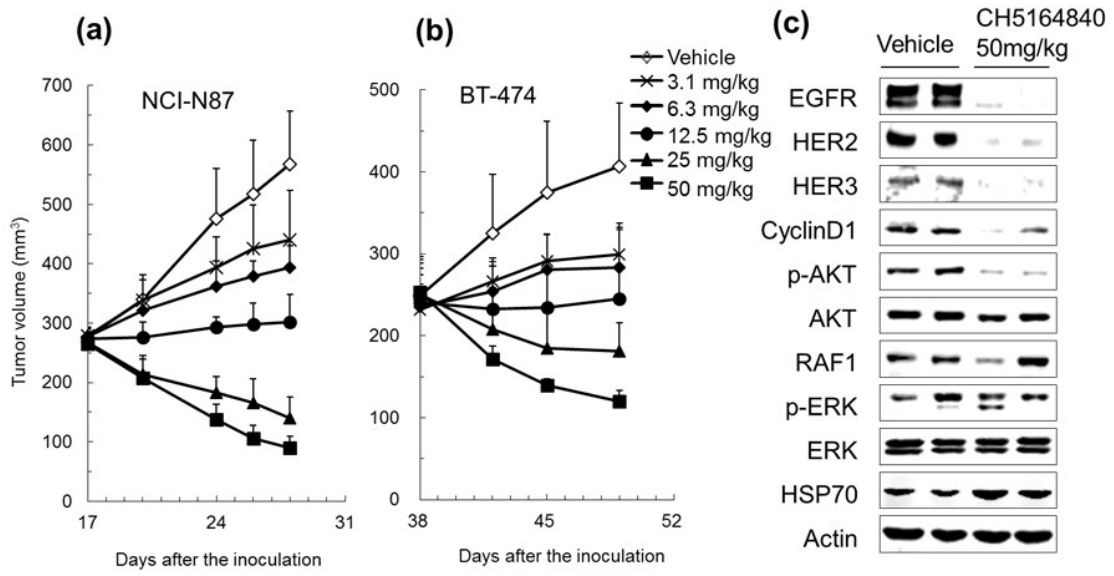

Fig. 1- 4. CH5164840 efficacy against HER2−overexpressing NCI-N87 and BT-474 xenograft models.

Mice bearing HER2-overexpressing tumors were orally administered the indicated doses of CH5164840 daily for 11 consecutive days. Mean tumor volume is shown. (a) NCI-N87 and (b) BT-474. Data are shown as mean ± SD (*n* = 4-5). (c) Lysates were prepared from the tumor and analyzed using Western blotting. p-, phospho.

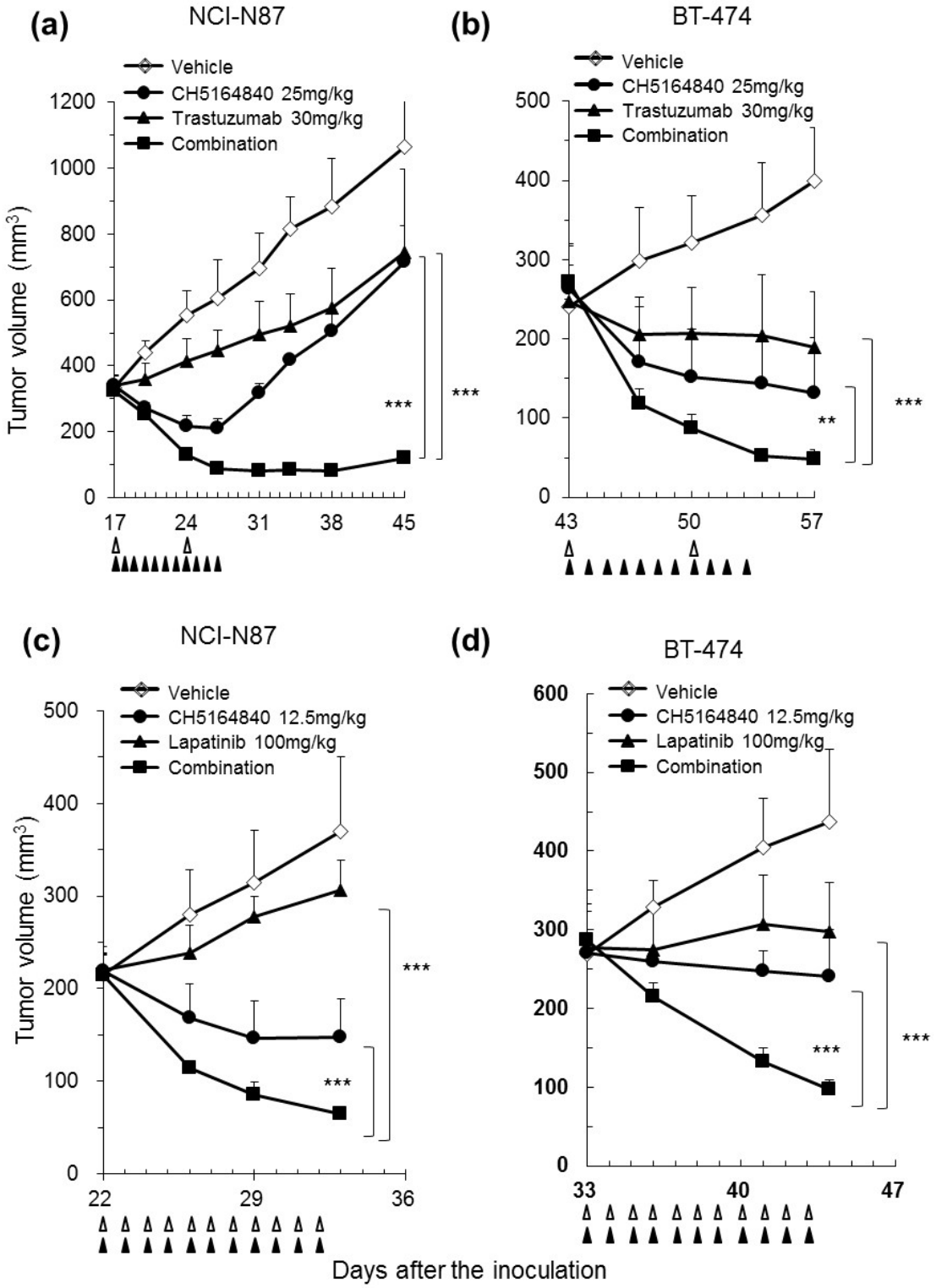

Fig. 1- 5. Combination therapy with CH5164840 enhanced antitumor efficacy against HER2-overexpressing NCI-N87 and BT-474 xenograft models.

(a) Mice bearing NCI−N87 tumors were orally administered 25 mg/kg CH5164840 daily for 11

consecutive days (indicated by black arrows) and/or intraperitoneally injected with 30 mg/kg trastuzumab once weekly for 2 weeks (indicated by white arrows). Mean tumor volumes were measured for over 4 weeks from treatment commencement. (b) Mice bearing BT−474 tumors were orally administered 25 mg/kg CH5164840 daily for 11 consecutive days (indicated by black arrows) and/or intraperitoneally injected with 30 mg/kg trastuzumab once weekly for 2 weeks (indicated by white arrows). (c, d) Mice bearing the HER2−overexpressing tumors NCI−N87 (c) or BT−474 (d), were orally administered 12.5 mg/kg CH5164840 daily for 11 consecutive days (indicated by black arrows) and/or orally administered 100 mg/kg lapatinib (indicated by white arrows). Data are shown as mean ± SD (n = 5).

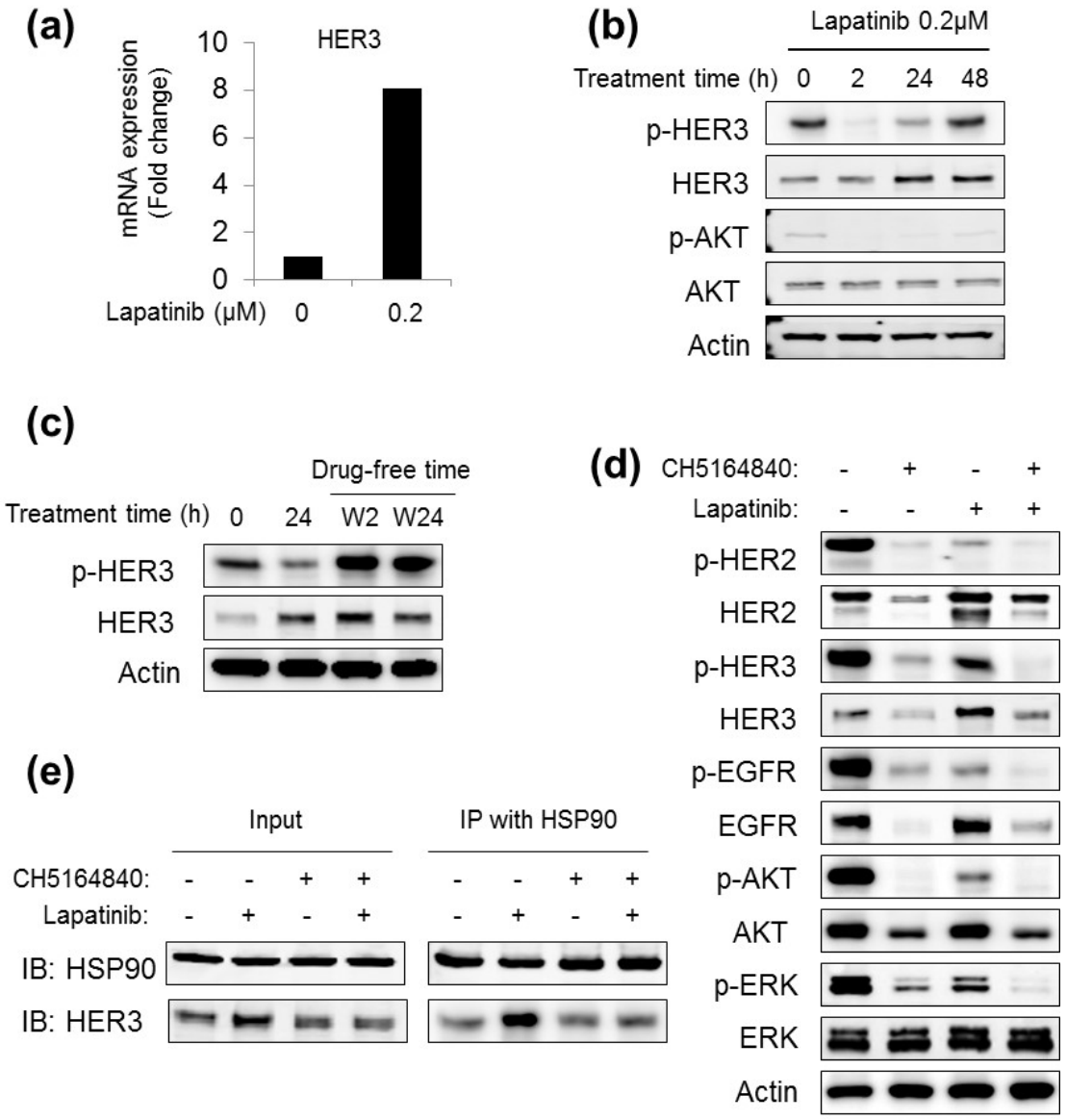

Fig. 1- 6. CH5164840 suppressed lapatinib treatment-induced HER3 signal activation *in vitro*.

(a) The relative expression of HER3 mRNA in NCI-N87 cells treated with 0.2 μM lapatinib was evaluated via real-time RT-PCR analysis of total RNA with an HER3-specific primer and normalized to the housekeeping gene (GAPDH). Relative expression is displayed as the fold change relative to the untreated control of the value for DMSO control lysate. (b) NCI-N87 cells were treated with 0.2 μM lapatinib for 2, 24, or 48 h. The cells were then lysed and analyzed via Western blotting with the indicated antibodies. (c) NCI-N87 cells were treated with 0.2 μM lapatinib for 24 h, washed with PBS, and then incubated with fresh medium for 2 or 24 h. The cells were then lysed and analyzed via Western blotting with the indicated antibodies. (d) NCI-N87 cells were treated with 1 μM CH5164840

and/or 0.2 μM lapatinib for 48 h, lysed, and analyzed via Western blotting with the indicated antibodies. (e) NCI-N87 cells were treated with 1 μM CH5164840 and/or 0.2 μM lapatinib for 24 h. The cells were then lysed, subjected to immunoprecipitation with the HSP90 antibody, and analyzed using Western blotting with the indicated antibodies. IP, immunoprecipitation.

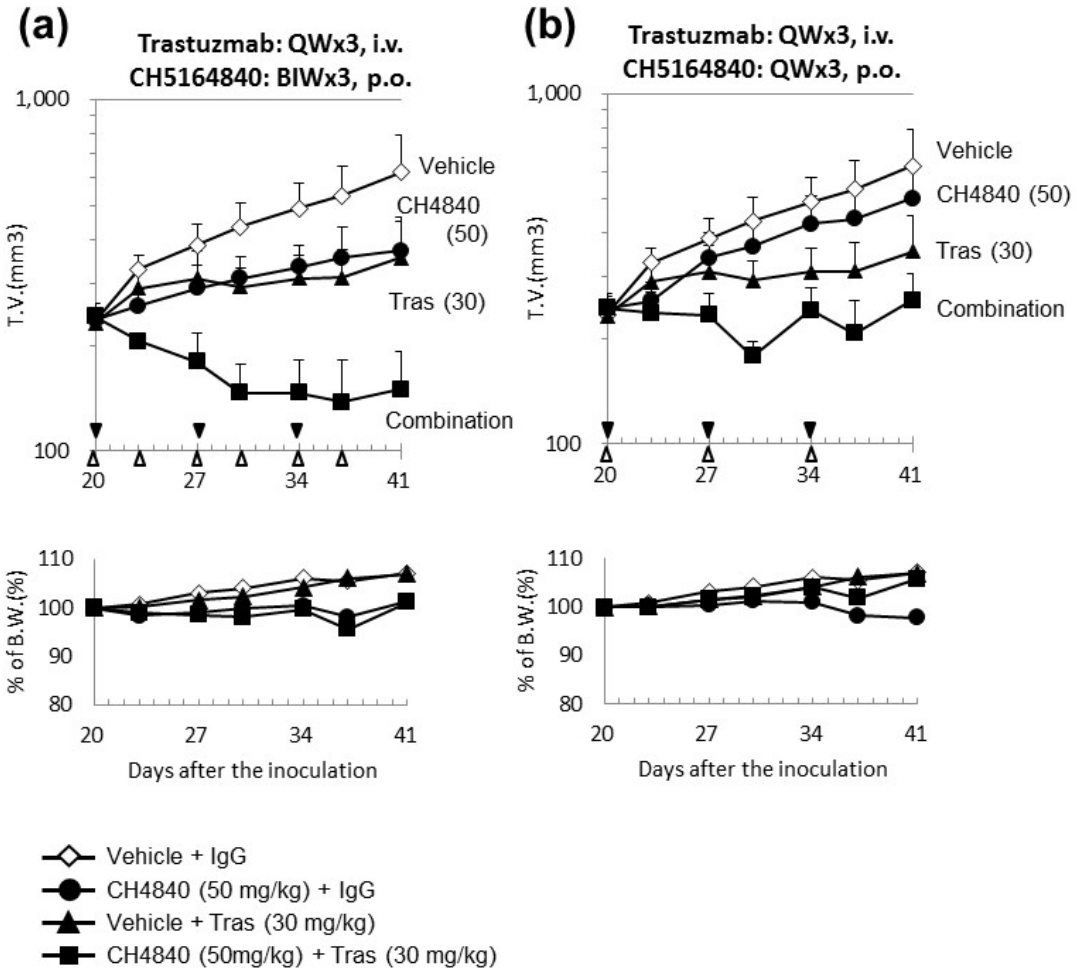

Fig. 1- 7. Study of the CH5164840 administration schedule during combination therapy with trastuzumab against HER2-overexpressing NCI-N87 xenograft models.

Mice bearing NCI-N87 tumors were orally administered (a) 50 mg/kg CH5164840 (CH4840) twice weekly (BIW) (indicated by white arrows) or (b) 50 mg/kg CH5164840 once weekly (QW) (indicated by white arrows), and intraperitoneally injected with 30 mg/kg trastuzumab (Tras) once weekly for 3 weeks (indicated by black arrows). Mean tumor volumes were measured for over 3 weeks from treatment commencement. Data are shown as mean ± SD (n = 4).

Chapter 2

Enhanced antitumor activity of erlotinib in combination with the HSP90 inhibitor CH5164840, against non-small-cell lung cancer

1. Introduction

Epidermal growth factor receptor (EGFR) plays a key role in non-small-cell lung cancer (NSCLC) development and progression. Two tyrosine kinase inhibitors (TKI) against EGFR – erlotinib and gefitinib – are currently available for NSCLC therapy. Although targeted inhibition of EGFR has shown promising initial clinical efficacy in the treatment of patients with NSCLC, which have exon 19 (DE 746-A750) and 21 (L858R)-activating EGFR mutations (44-46), primary and acquired resistance to these drugs in some patients is an obstacle to treatment efficacy (47). The major mechanisms of resistance to TKI are EGFR mutations (48), MET amplification (49), hepatocyte growth factor (HGF) activation (50), phosphatase and tensin homolog (PTEN) loss (51) and other genomic alterations with wild-type EGFR, including KRAS mutations (48, 52) and ALK-fusion proteins (53). Additionally, adenocarcinoma with sensitive EGFR mutations can transform into small cell lung cancer (SCLC) in the process of acquiring resistance to EGFR-TKIs (54). A secondary mutation in the EGFR gene (T790M) is the major cause of resistance to gefitinib and erlotinib (55, 56), and is found in 50% of clinically resistant patients (57). Due to the potential for resistance to TKI in EGFR-addicted tumors, identification of an effective treatment using rationalized combinations of agents is particularly promising.

EGFR is one of the most potent oncogenic client proteins of HSP90. Furthermore, mutated EGFR seems to be more sensitive than wild-type EGFR to degradation from HSP90 inhibition (23, 24). These unique features are expected to overcome the problem of resistance to TKI. STAT3 is also an HSP90 client protein (58) and an important signaling mediator for EGFR. It is activated in approximately 50% of NSCLC primary tumors and lung cancer cell lines (59-61), and this pathway is upregulated in NSCLC cells harboring EGFR mutations (62). Janus kinase (JAK), upstream of STAT3, is also an HSP90 client, and the JAK-STAT pathway is involved in immune function, cell growth, differentiation, hematopoiesis, and tumor growth.

Recently, a novel potent HSP90 inhibitor: CH5164840, was identified. The present study elucidates the *in vitro* and *in vivo* properties of CH5164840 alone and in combination with erlotinib, including its antitumor activity in EGFR overexpressing and erlotinib-resistant NSCLC xenograft models.

2. Materials and Methods

2- 1. Compounds

CH5164840 was synthesized by Chugai Pharmaceutical Co., Ltd (Kanagawa, Japan) (33). Erlotinib was obtained from Chugai Pharmaceutical／F. Hoffmann-La Roche (Basel, Switzerland).

2- 2. Cell lines

The human NSCLC cell lines HCC827, NCIH292, NCI-H1781, A549, NCI-H1650, NCI-H1975 and NCI-H441, were obtained from the American Type Culture Collection (Manassas, VA, USA). The human NSCLC cell line EBC-1 was obtained from RIKEN Cell Bank (Ibaraki, Japan). The human NSCLC cell line PC-9 was obtained from Immuno-Biological Laboratories (Fujioka, Japan). All cell lines were maintained according to the supplier's instructions.

2- 3. Cell culture

For proliferation assays, tumor cells were seeded into microtiter plates containing compounds and incubated at 37°C in 5% CO_2. After incubation for 4 days, a Cell Counting Kit-8 solution (Dojindo Laboratories, Kumamoto, Japan) was added and absorbance measured at 450 nm with a Microplate- Reader iMark (Bio-Rad Laboratories, Hercules, CA, USA). Anti-proliferative activity was calculated using the formula: $(1-T/C) \times 100$ (%), where T represents the absorbance of drug-treated cells and C represents that of untreated control cells at 450 nm. The IC_{50} values were calculated using Microsoft Excel 2007 (Redmond, WA, USA). Caspase-3/7 activity and cell viability were measured with the Caspase-Glo 3/7 Assay Kit (Promega, Madison, WI, USA) and CellTiter-Glo Luminescent Cell Viability Assay (Promega), respectively, using EnVision High Throughput Screening (PerkinElmer, Waltham, MA, USA).

2- 4. Western blotting

Western blotting was performed as described in chapter 1. Primary antibodies were used for pY1068-EGFR, EGFR (L858R), pS473-AKT, AKT, pT202/Y204-ERK, ERK, pY705-STAT3, STAT3, JAK1, JAK2 and tyrosine kinase 2 (TYK2) (Cell Signaling, Beverly, MA, USA), EGFR, HER2, MET, RAF1, actin, GAPDH and Histone H1 (Santa Cruz Biotechnology, Santa Cruz, CA, USA) and HSP70 and HSP90 (Stressgen, Victoria, Canada). Signals were developed using ECL Plus (GE Healthcare, Buckinghamshire, UK), followed by LAS- 4000 (Fujifilm, Tokyo, Japan) or the Odyssey Infrared Imaging System (LI-COR Biosciences, Lincoln, NE, USA).

2- 5. RNA interference

Cells were seeded onto a 96-well plate and transfected with Human STAT3, JAK1, JAK2 and TYK2 ON-TARGETplus SMARTpool ORF and ON-TARGETplus Non-targeting Pool (Thermo

Scientific, Dharmacon, Waltham, MA, USA) using Lipofectamine RNAiMAX (Invitrogen, Carlsbad, CA, USA), and treated with 0.2 μM erlotinib. At 96 h after siRNA transfection, cell viability was determined using the CellTiter-Glo luminescent cell viability assay (Promega).

2- 6. Xenograft models and efficacy studies

All animal studies were approved by the Chugai Institutional Animal Care and Use Committee. Cancer cells (0.5–1.0 x 10^7) were implanted subcutaneously into the right flank of athymic nude (BALB／c nu／nu) mice (Charles River Laboratories, Kanagawa, Japan). Tumor volume (TV) was calculated using the formula TV = $ab2 / 2$, where a and b represent tumor length and width, respectively. Once the tumors reached a volume of approximately 200–300 mm^3, THE animals were randomized into each group (n = 4–5) and treatment was initiated. CH5164840 was dissolved in a vehicle of 10% DMSO/10% Cremophor EL/ 0.02 N HCl in water. CH5164840 and erlotinib were orally administered once daily for 11 days. Tumor growth inhibition (TGI) was calculated using the formula TGI = $(1-[T_t-T_0]/[C_t-C_0]) \times 100$ (%), where T (TV of treated group; T_0 on day 0 or T_t on day t) and C (TV of control group; C_0 on day 0 or C_t on day t) represent mean tumor volume. The maximum tolerated dose was defined as the dose that resulted in neither lethality nor more than 20% bodyweight loss. For pharmacodynamic studies, blood was collected 4 h after the last administration of CH5164840 and PBMC were prepared with M-SMF (JIMRO, Gunma, Japan), lysed, and analyzed using Western blotting.

2- 7. Statistical analysis

For *in vivo* combination studies, SAS preclinical package v5 software (SAS Institute, Cary, NC, USA) was used for statistical analyses (Tukey's test). For *in vitro* experiments, statistical values were defined using the Student's *t*-test.

3. Results

3- 1. Novel HSP90 inhibitor CH5164840, has potent growth inhibitory activity against NSCLC *in vitro* and antitumor activity *in vivo*

Recently, through virtual screening and structure-based drug design, CH5164840 was identified as an HSP90 inhibitor with a novel chemical structure (32, 33). It was demonstrated to show antitumor-activity against HER2 positive-tumors in mono- and combination-therapies with HER2-targeted agents (63). In this study, the potency of CH5164840 against NSCLC was examined. In an initial evaluation, the *in vitro* cell growth inhibition of CH5164840 or erlotinib was examined to determine the sensitivity of NSCLC cell lines with various genotypes, including PC-9 and HCC827 (EGFR ΔE746-A750), NCI-H292 (wild-type EGFR overexpression), NCI-H1975 (EGFR T790M and L858R mutant), NCI-H1650 (EGFR ΔE746-A750, PTEN null), NCI-H1781 (HER2

G776insV_G/C mutant), and A549 (KRAS mutant). The IC_{50} values of CH5164840 were found to be 140–550 nM in seven NSCLC cell lines, regardless of genetic mutations, although sensitivities to erlotinib were more variable (IC_{50} values, 4.7–13000 nM; Table 2-1). Next, the degradation of HSP90 client proteins in NSCLC cell lines by CH5164840 was examined. CH5164840 was found to significantly reduce EGFR, HER2, and MET protein levels, and suppress downstream AKT and ERK signaling (Fig. 2-1). The induction of HSP70, a marker of HSP90 inhibition, was also confirmed. To evaluate the *in vivo* antitumor activity of CH5164840, several xenograft studies were conducted using NSCLC cell lines in nude BALB/c mice. Daily oral administration of CH5164840 resulted in a significant dose-dependent antitumor activity in the NCI-H1650 (EGFR mutant, PTEN null) xenograft models, with a maximum TGI of 131% (Fig. 2-2a, Table 2-2). Additionally, we confirmed the dose-dependent induction of HSP70 in murine peripheral blood mononuclear cells (PBMC), which is a marker of HSP90 inhibition (Fig. 2-2b). Like NCI-H1650 antitumor activity, CH5164840 showed substantial antitumor activity in NCI-H292 (wild-type EGFR overexpression), NCI-H1975 (EGFR mutant) and NCI-H441 (wild-type EGFR, MET overexpression) xenograft models (Table 2-1). In all *in vivo* studies, the doses of CH5164840 tested were well tolerated, with no gross toxicity observed in the treated animals. Collectively, these data show that CH5164840 inhibited HSP90, resulting in the inhibition of *in vitro* cell growth and *in vivo* antitumor activity against multiple NSCLC cell lines.

3- 2. CH5164840 enhances the antitumor activity of erlotinib in a NCI-H292 wild-type EGFR overexpression, erlotinib-halfway sensitive model

Due to the moderate activity of erlotinib against NCI-H292 NSCLC cells, the effect of CH5164840 on erlotinib activity against NCI-H292 cells, which overexpress wild-type EGFR, was investigated. To confirm the cellular effects of this combination treatment *in vitro*, cell growth inhibition and caspase-3/7 activity were evaluated. As shown in Fig. 2-3a, CH5164840 enhanced the cell growth inhibitory activity of erlotinib. Further, when NCI-H292 cells were treated with a combination of erlotinib and CH5164840, CH5164840 significantly enhanced the caspase-3/7 activity of erlotinib (Fig. 2-3b). To examine the combined antitumor activity of CH5164840 and erlotinib *in vivo*, 25 mg/kg of erlotinib and/or 12.5 mg/kg of CH5164840 was administered to the NCI-H292 xenograft models. CH5164840 synergistically enhanced the antitumor activity of erlotinib (Fig. 2-3c). Erlotinib and CH5164840 co-therapy produced a statistically significant effect on TGI, compared with monotherapy with either, causing tumor regression. These data support the effectiveness of a combination strategy using erlotinib and CH5164840 against EGFR-overexpressing NSCLC. Next, the molecular mechanisms of the synergistic effect of erlotinib and CH5164840 co-therapy in NCI-H292 cells were examined. Firstly, the effect of these agents on cell signaling was analyzed via Western blotting. Erlotinib and CH5164840 co-therapy reduced EGFR and phospho-EGFR protein levels and

suppressed downstream AKT and ERK signaling (Fig. 2-4a). Additionally, erlotinib resulted in a dose-dependent increase in STAT3 phosphorylation compared with DMSO control (Fig. 2-4b), which was mainly present in the nucleus (Fig. 2-4c). Interestingly, co-treatment with CH5164840 and erlotinib reduced the phosphorylation level of STAT3 (Fig. 2-4c).

JAK1reportedly phosphorylates STAT3 in NSCLC cells (64). It was confirmed that siRNA knockdown of JAK1, but not its family protein JAK2 or TYK2, inhibited erlotinib-induced STAT3 phosphorylation in NCI-H292 cells (Fig. 2-4d). Additionally, HSP90 inhibition by CH5164840 induced degradation of the JAK1 protein (Fig. 2-4a). Further, to explore the effect of JAK1 and STAT3 on cell growth, their knockdown by siRNA was examined. Inhibition of STAT3 expression by siRNA specifically enhanced cell growth inhibition by erlotinib (Fig. 2-4e), producing statistically significant results. Combined knockdown of erlotinib and JAK1 led to more effective cell growth inhibition compared to STAT3 (Fig. 2-4e). Collectively, these findings suggest that in addition to AKT and ERK signaling, suppression of the JAK1-STAT3 signaling pathway by CH5164840 enhanced the antitumor effects of erlotinib in NSCLC.

3- 3. CH5164840 enhances the antitumor activity of erlotinib in an erlotinib-resistant NCI-H1975 model

The effect of erlotinib and CH5164840 co-treatment were further explored using NCI-H1975 NSCLC cells. NCI-H1975 cells harbor the EGFR T790M gatekeeper mutation, which modulates the accessibility of the kinase ATP-binding pocket, a secondary EGFR mutation that is a major cause of resistance to erlotinib. To investigate the combined effect of erlotinib and CH5164840, the anti-proliferative effect of the agents on NCI-H1975 cells were examined. CH5164840 enhanced the cell growth-inhibitory and caspase-3/7 activities of erlotinib (Figs. 2-5a, b). The *in vivo* antitumor activity of this combination therapy against human tumor xenograft models in mice was then investigated. When a combination of 25 mg/kg erlotinib and 25 mg/kg CH5164840 was orally administered to a NCI-H1975 xenograft model, tumor growth was significantly inhibited, despite erlotinib treatment alone having no effect (Fig. 2-5c). The enhanced antitumor activity with combination therapy was statistically significant compared with monotherapy with either, and no gross toxicity was observed in any of the treated animals. Additionally, combination therapy resulted in reduced protein levels of mutated EGFR, JAK1, phospho-STAT3, phospho-AKT, and phospho-ERK (Fig. 2-5d). These results suggest that CH5164840 potentiates the efficacy of erlotinib in an erlotinib-resistant model harboring the EGFR T790M gatekeeper mutation.

4. Discussion

EGFR is an attractive anticancer therapy target because it plays an important role in lung carcinogenesis. Moreover, its expression is correlated with poor prognosis (65) and EGFR-TKI,

erlotinib, and gefitinib, have shown a clinical response in NSCLC with activating EGFR mutations. However, the development of primary and acquired resistances to these drugs over several years has become a major clinical problem. Recently, many resistant mechanisms of EGFR-TKI have been investigated (66), including EGFR mutations T790M (48, 67), MET amplification (49), hepatocyte growth factor (HGF) activation (50), PTEN loss (51, 68) and AXL activation (69). To overcome TKI resistance, corresponding strategies for each TKI-resistant mechanism are needed. The combination of a TKI and an HSP90 inhibitor is considered particularly promising because the inhibition of HSP90 induces degradation of molecules involved in TKI resistance, including mutant EGFR, MET, and EML4-ALK. HSP90 inhibitors have shown efficacy against established EGFR-TKI–resistant cells, EGFR T790M (70), and HGF overexpression (71). In fact, the HSP90 inhibitor IP-504, has shown clinical activity in patients with ALK rearrangement in a phase 1／2 study (72). CH5164840, an HSP90 inhibitor with a novel chemical structure, can be taken orally and exhibits highly potent antitumor efficacy (63). In the present study, it inhibited cell growth in NSCLC cell lines with different oncogenic drivers, induced degradation of representative HSP90 client proteins: EGFR, HER2, MET and RAF1, and inhibited the phosphorylation of downstream signaling proteins AKT and ERK. Treatment with CH5164840 also induced HSP70 expression. Generally, studies on HSP90 inhibitors focus on the degradation of client proteins or induction of HSP70 as a biomarker for the HSP90 inhibitor. However, induction of HSP70 by HSP90 inhibition has been shown to reduce the antitumor effect of HSP90 inhibitors, and knockdown of HSP70 by siRNA increased 17-AAG-induced apoptosis (73). Therefore, abrogating HSP70 induction approaches are raised to increasing the sensitivity of HSP90 inhibitors (74).

Furthermore, CH5164840 monotherapy showed antitumor activity against NSCLC xenograft models; CH5164840 showed antitumor activity against a NCI-H441 (wild-type EGFR and MET overexpression) model. Therefore, it is considered useful for patients who exhibit MET-associated TKI resistance. In fact, as shown in Fig. 2-6, this was confirmed in NCI-H441 and EBC-1 (MET amplification) cells, in which erlotinib did not show cell growth inhibition, which CH5164840 enhanced the cell growth inhibitory activity of erlotinib with IC_{50} values of erlotinib in the individual cell lines of >20 μM (EBC-1) and 10.0 μM (NCI-H441) *in vitro*. Furthermore, combination treatment resulted in degradation of phosphorylated and total EGFR or MET in these cells. Collectively, these results show that the HSP90 inhibitor is a potential therapeutic option in combination with erlotinib against TKI-resistant NSCLC with aberrant c-MET. Similarly, it may also be effective in patients with PTEN loss, which is one of the mechanisms of TKI resistance, because of the antitumor activity of CH5164840 in the NCI-H1650 (EGFR DE746-A750, PTEN null) model. These results show that the novel HSP90 inhibitor CH5164840, has potent antitumor activity *in vitro* and *in vivo* against clinically relevant NSCLC, including erlotinib-resistant models. The association between EGFR protein expression levels and clinical response to EGFR-TKI has

been variable (75, 76), and, in fact, erlotinib elicits only a moderate response against wild-type EGFR-overexpressing NCI-H292 cells. In the present study, treatment of NCI-H292 cells with a combination of EGFR-TKI erlotinib and the HSP90 inhibitor CH5164840, was shown to lead to synergistic cell growth inhibition and apoptosis induction. These *in vitro* results were consistent with the regression of antitumor activity by combination therapy in a NCI-H292 xenograft model. Further, the molecular mechanisms by which CH5164840 enhanced the efficacy of erlotinib was examined. Combination therapy with erlotinib and CH5164840 reduced EGFR and phospho-EGFR levels, as well as that of downstream signaling proteins AKT and ERK. Interestingly, it was noticed that erlotinib treatment increased phospho-STAT3 in NCI-H292 cells, an effect that was strongly suppressed by CH5164840. The sensitivity of erlotinib-induced phospho-STAT3 is sensitive to HSP90 inhibition is most likely because STAT3 is a client protein of HSP90 (58). Therefore, in NCI-H292 cells, the efficacy of erlotinib might be increased through blocking STAT3 signaling by HSP90 inhibition. STAT3 can be activated through multiple pathways, including EGFR, the IL-6／gp130 receptor family, platelet-derived growth factor receptor (PDGFR), Src kinase, and JAK. JAK1 reportedly causes STAT3 activation in NSCLC cells (64), which was confirmed in the present study, together with the fact that both basal- and erlotinib-induced phospho-STAT3 were inhibited by JAK1 knockdown with siRNA, but not JAK2 and TYK2 knockdown (Fig. 2-4d). Although a combination of erlotinib treatment and JAK1 knockdown is more effective for cell growth inhibition than that of erlotinib treatment and STAT3 knockdown, the former does not completely inhibit cell growth. Therefore, additional blocking of the AKT and ERK pathways by an HSP90 inhibitor might be an important therapeutic approach in NCI-H292 NSCLC cells. However, the mechanism by which phospho-STAT3 is increased by erlotinib-induced EGFR inhibition remains unknown. Further investigation is needed to clarify the upstream pathways of EGFR TKI treatment-induced STAT3 activation. Acquired resistance to TKI, usually owed to the development of a second point mutation (T790M) in EGFR, is also a serious clinical problem. Consistent with other HSP90 inhibitors (77, 78), CH5164840 monotherapy shows antitumor activity against NCI-H1975 NSCLC cells harboring EGFR L858R and T790M mutations. Additionally, erlotinib and CH5164840 co-therapy showed significant synergism, despite the lack of an antitumor activity by erlotinib monotherapy in this model. Further, combination therapy simultaneously induced degradation of mutant EGFR, phospho-EGFR, and downstream AKT, ERK, and STAT3 signaling. As such, combination therapy with TKI and an HSP90 inhibitor might be useful in preventing TKI resistance development, as most TKIs are at potential risk of encountering TKI resistance and addicted-oncogenic proteins are degraded by HSP90 inhibition (55). In conclusion, these data highlight the benefits of using an HSP90 inhibitor in combination with EGFR-targeted therapies for the treatment of EGFR-addicted NSCLC, and supports the clinical development of this co-therapy.

5. Tables

Table 2- 1. Anti-proliferative activity of CH5164840 in non−small−cell lung cancer cell lines

Cell lines	EGFR status	CH5164840 IC_{50} (μM)	Erlotinib IC_{50} (μM)
PC-9	E746_A750del	0.16	0.0048
HCC827	E746_A750del	0.14	0.0047
NCI-H292	WT overexpression	0.49	0.16
NCI-H1781	WT	0.55	1.7
A549	WT	0.19	3.4
NCI-H1650	E746_A750del	0.16	4.1
NCI-H1975	L858R & T790M	0.30	13

Table 2- 2. Antitumor efficacy of CH5164840 in tumor xenograft models at MTD

Models	Tumor types	Status	Client	MTD (mg/kg)	TGI (%)
NCI-H292	Mucoepidermoid	EGFR overexpression	EGFR	25	92
NCI-H441	Papillary adeno	MET overexpression	MET	50	115
NCI-H1975	Adenocarcinoma	EGFR mutant	EGFR L858R & T790M	50	112
NCI-H1650	Adenocarcinoma	EGFR mutant	EGFR E746-A750del	50	131

EGFR, epidermal growth factor receptor; MET, met proto-oncogene; MTD, maximum tolerated dose; TGI, tumor growth inhibition. CH5164840 was orally administered once daily for 11 days.

6. Figures

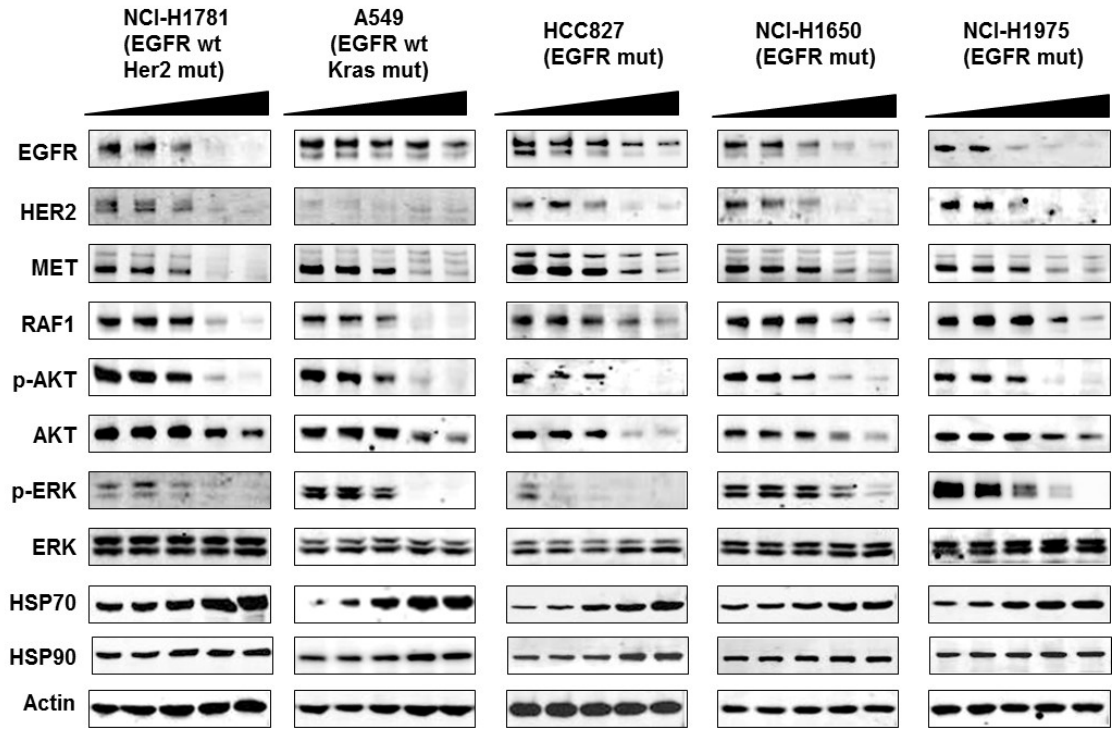

Fig. 2- 1. CH5164840 induces degradation of multiple HSP90 client proteins in non−small−cell lung cancer (NSCLC) cell lines.

NSCLC cell lines were treated with 0, 0.04, 0.2, 1, or 5 μM CH5164840 for 24 h, lysed, and analyzed using Western blotting with indicated antibodies.

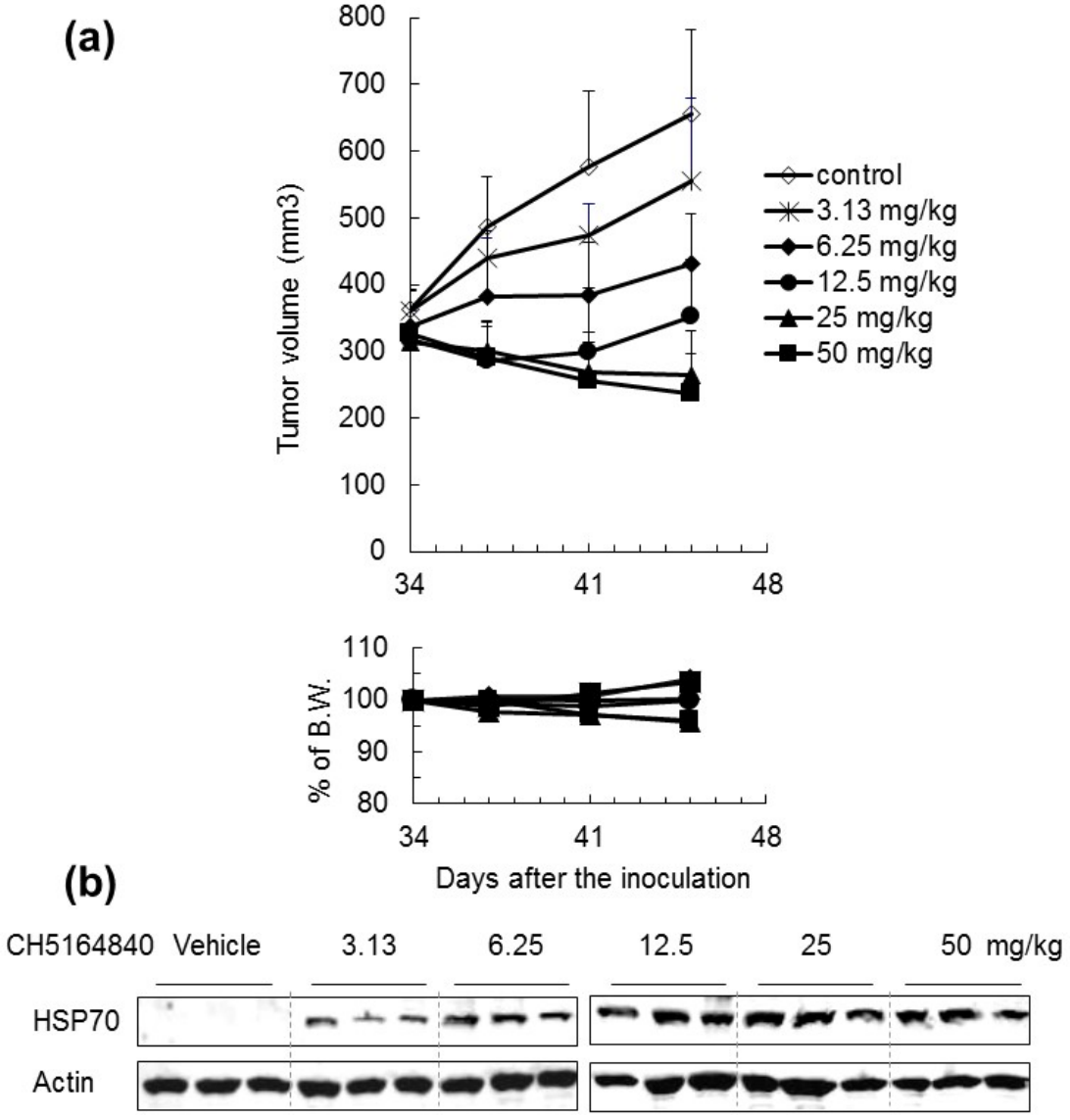

Fig. 2- 2. Antitumor activity of CH5164840 in a NCI−H1650 erlotinib−resistant xenograft model and the pharmacodynamic response.

(a) Mice bearing NCI-H1650 tumors were orally administered the indicated doses of CH5164840 daily for 11 consecutive days. Mean tumor volume is shown. Data are shown as mean ± SD (n = 4-5). (b) Four hours after the final administration in (a), murine PBMC were isolated from blood, lysed, and analyzed using Western blotting.

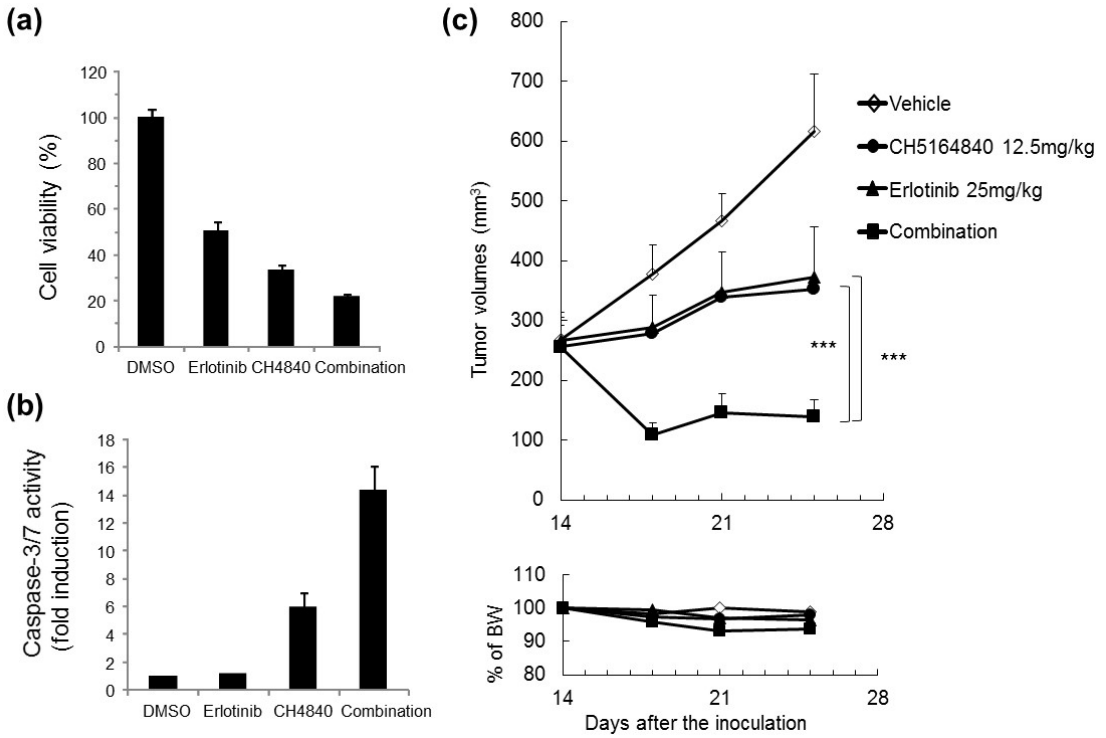

Fig. 2- 3. Antitumor activity of CH5164840 in combination with erlotinib on NCI−H292 EGFR−overexpressing NSCLC *in vitro* and *in vivo*.

(a, b) NCI-H292 cells were treated with 0.2 μM erlotinib and/or 0.5 μM CH5164840 for 48 h (for caspase-3/7 activity and cell viability) and 96 h (for cell viability). Caspase-3/7 activity and cell viability were measured with the Caspase-Glo 3/7 assay and CellTiter-Glo, respectively, using EnVision High Throughput Screening. Caspase-3/7 activity was normalized to cell viability. (c) Mice bearing NCI-H292 tumors were orally administered 12.5 mg/kg CH5164840 daily for 11 consecutive days and/or 25 mg/kg erlotinib. Data are shown as mean ± SD (n = 5). Tukey's test: ***P < 0.001.

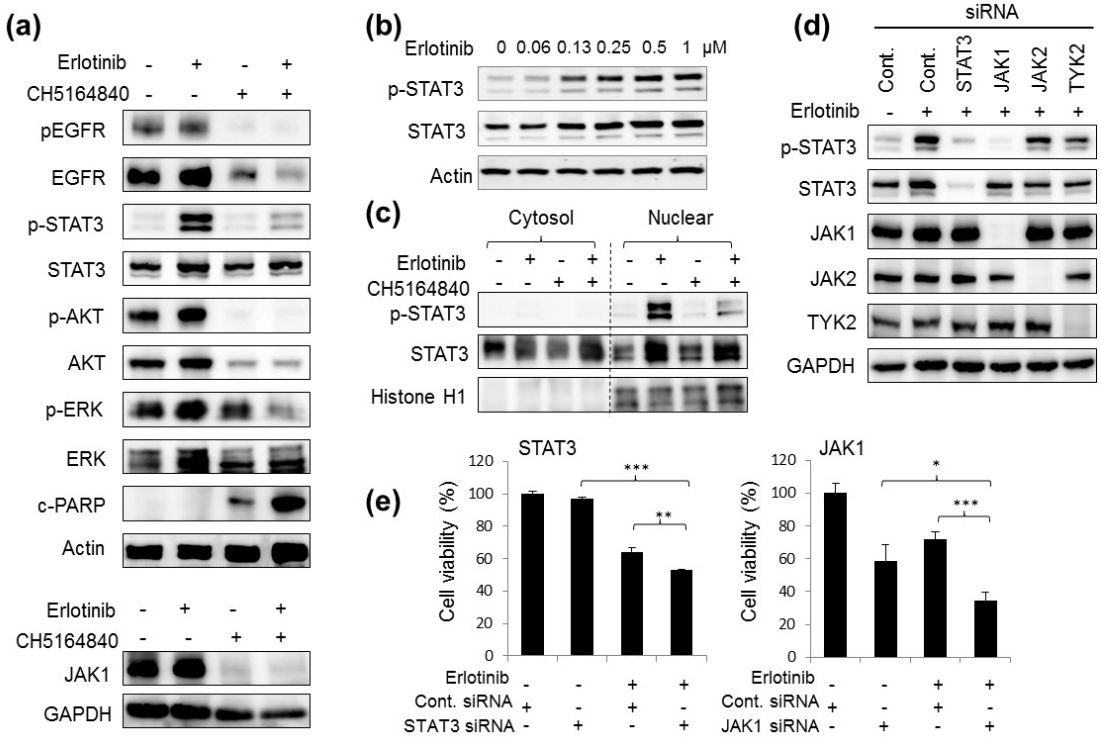

Fig. 2- 4. CH5164840 treatment suppressed erlotinib−induced STAT3 signaling in NCI−H292 cells.

(a) NCI-H292 cells were treated with 0.2 μM erlotinib and/or 0.5 μM CH5164840 for 48 h, lysed, and analyzed using Western blotting. (b) NCI-H292 cells were treated with the indicated concentration of erlotinib for 24 h and their STAT3 and phospho-STAT3 protein content analyzed. (c) NCI-H292 cells were treated with 0.2 μM erlotinib and/or 0.5 μM CH5164840 for 48 h, and their cytosol and nuclear fractions analyzed using Western blotting. Histone H1 indicates loading control for nuclear fraction. (d) NCI-H292 cells were transfected with 10 nM STAT3, JAK1, JAK2, TYK2, or control siRNA. At 24 h post-transfection, cells were treated with 0.2 μM erlotinib, cultured for 24 h, lysed, and analyzed using Western blotting. (e) NCI-H292 cells were transfected with 10 nM STAT3 siRNA, JAK1 siRNA, or control siRNA, and treated with DMSO or 0.2 μM erlotinib. At 96 h post-transfection, cell viability was determined using CellTiter-Glo. Data are shown as mean ± SD (n = 3). Student's t-test: *P < 0.05; **P <0.01; ***P < 0.001. c-PARP, cleaved poly (ADP-ribose) polymerase; p, phospho; −, DMSO; +, compound.

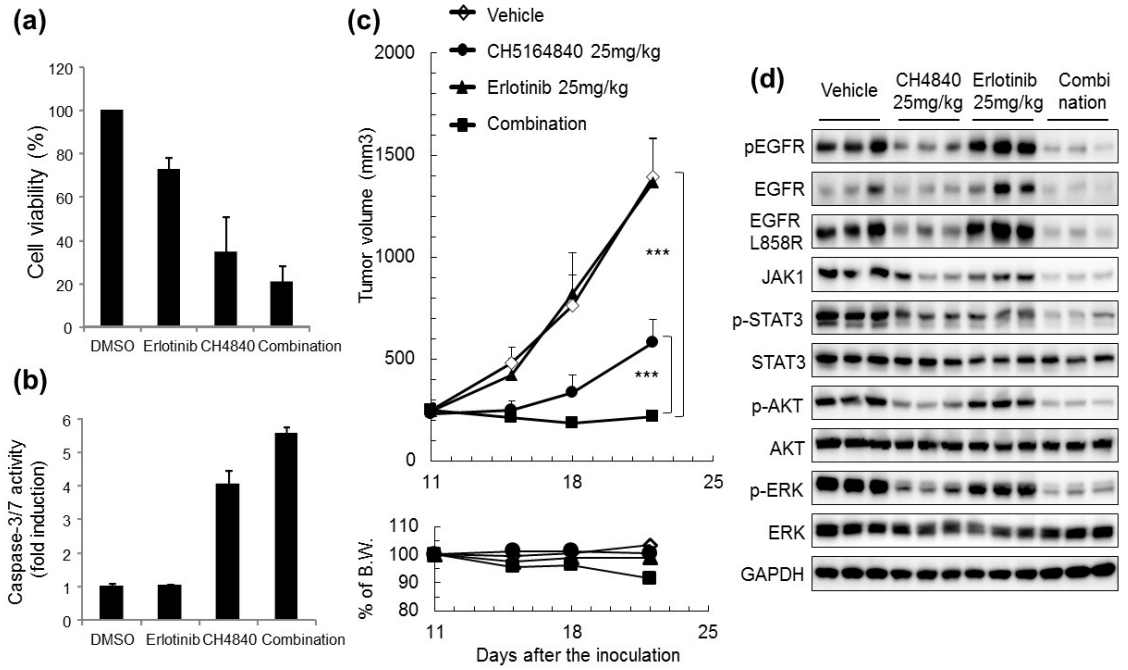

Fig. 2- 5. Antitumor activity of CH5164840 in combination with erlotinib in a NCI−H1975 erlotinib−resistant model.

(a, b) NCI−H1975 cells were treated with 1 μM erlotinib and/or 1 μM CH5164840 for 48 h (for caspase−3/7 activity and cell viability) and 96 h (for cell viability). Caspase−3/7 activity and cell viability were measured with the Caspase−Glo 3/7 assay and CellTiter−Glo, respectively, using EnVision High Throughput Screening. Caspase activity was normalized to cell viability. (c) Mice bearing NCI−H1975 tumors were orally administered 25 mg/kg of CH5164840 and/or 25 mg/kg of erlotinib daily for 11 days. (d) Four hours after the final administration in (c), tumors were resected, lysed, and analyzed using Western blotting. p, phospho. Data are shown as mean ± SD (n = 4-5) Tukey's test: ***P < 0.001.

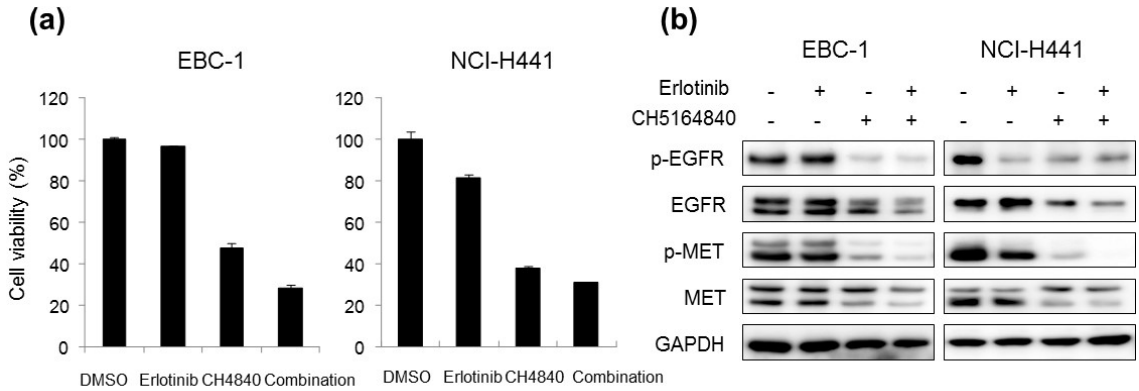

Fig. 2- 6. Antitumor activity of CH5164840 in combination with erlotinib on NSCLC with aberrant c-MET *in vitro*.

(a) EBC-1 cells were treated with 1 μM erlotinib and/or 0.2 μM. CH5164840 and NCI-H441 cells were treated with 1 μM erlotinib and/or 0.5 μM CH5164840 for 96 h. Cell viability was measured with the CellTiter-Glo, using EnVision High Throughput Screening. Data are shown as mean ± SD (*n* = 3) (b) EBC-1 cells were treated with 1 μM erlotinib and/or 0.2 μM CH5164840, and NCI-H441 cells were treated with 1 μM erlotinib and/or 0.5 μM CH5164840 for 48 h, lysed, and analyzed using Western blotting.

General discussion

HSP90 is considered as an attractive anticancer therapy target for several reasons. Firstly, its role in the regulation of its client proteins, many of which are cancer-related proteins, including kinases, transcription factors, and steroid receptors. HSP90 inhibition induces degradation of these clients, leading to the inhibition of multiple signaling pathways that regulate tumor cell proliferation and survival. Such inhibition was observed in this study with the novel HSP90 inhibitor CH5164840, which induced multiple client degradation, followed by the suppression of multiple signaling pathways.

Another attractive feature of HSP90 as an antitumor target is the possibility of tumor selectivity (9). As shown in Fig. 1-3b, a higher binding affinity of bio-CH to tumor HSP90 compared to normal HSP90, was observed. This selective binding to HSP90 in tumor tissue HSP90 and its long retention in tumor tissue retention in the mouse model, allow CH5164840 to exert a potent antitumor activity. Furthermore, CH5164840 enhanced the antitumor efficacy of the HER2-targeted therapy trastuzumab and lapatinib, in the NCIN87 and BT-474 tumor models. In combination with trastuzumab in the NCI-N87 xenograft model, antitumor efficacy was sustained over the follow-up period without any additional administration. As shown in Fig. 1-6, examination of the molecular mechanisms behind the enhanced efficacy of CH5164840 was commenced by looking at HER3 induction by lapatinib in the NCI-N87 cells, in the same manner as that previously reported in SK-BR-3 cells (41). These observations indicate that the combination of the HSP90 inhibitor CH5164840, and HER2-targeted therapies might be helpful in treating tumors whose growth and survival depend on HSP90.

The first-generation EGFR-TKIs, erlotinib and gefitinib, have shown a clinical response in NSCLC with activating EGFR mutations. However, the development of primary and acquired resistances to these drugs for over several years has become a major clinical problem. The most common resistance mechanism of TKIs in EGFR mutant lung cancer is the T790M, which is found in 60% of patient with acquired resistance. Recently, many resistant mechanisms of EGFR-TKI have been investigated (66), and corresponding strategies for each TKI-resistant mechanism are needed to overcome resistance and prolong the efficacy of EGFR-targeted therapies. The second generation EGFR-TKI, afatinib, an irreversible HER family blocker (79), is also resistance to EGFR T790M mutant. The third generation EGFR-TKI, osimertinib, is selective for mutated forms of EGFR, including the common TKI-sensitizing L858R mutation and exon 19 deletions, and the acquired T790M resistance mutation (80, 81). However, osimertinib also became resistant to EGFR C797S mutation. Although many EGFR-TKIs are developed to overcome resistance and prolong the treatment period and progression-free survival, other resistant mechanism may appear during treatment. Heterogeneity is another TKI resistance mechanism and clinical treatment strategy problem.

The TKI and an HSP90 inhibitor combination therapy strategy is considered particularly promising in overcoming TKI resistance and may prolong the treatment period, because the inhibition of HSP90 induces degradation of molecules that are involved in TKI resistance, including mutant EGFR, MET

and EML4-ALK. CH5164840 showed antitumor activity against the erlotinib-resistant xenograft models: NCI-H441 (wild-type EGFR and MET overexpression), NCI-H1650 (EGFR DE746-A750, PTEN null), wild-type EGFR-overexpressing NCI-H292, and NCI-H1975 (EGFR L858R and T790M mutations). Therefore, it is considered useful for patients who exhibit various mechanism of TKI resistance. In fact, the HSP90 inhibitor IP-504, has shown clinical activity in patients with ALK rearrangement in a phase 1／2 study (72).

HSP90 is considered an attractive anticancer therapy target and HSP90 inhibitors have shown great antitumor efficacy in preclinical studies. Although in recent years, HSP90 inhibitors have been intensively developed, and some are currently in clinical trials as anticancer therapeutics (82), clinical developments of HSP90 inhibitors remains unsuccessful due to safety concerns. However, in these trials, the HSP90 inhibitors 17-DMAG (83), IPI-504 (72), PF-04929113 (SNX-5422) (84), NVP-AUY922 (85), and AT13387 (86), resulted in visual toxicity; this did not occur with the HSP90 inhibitors 17-AAG (87) and ganetespib (88). Although CH5164840 has attractive properties as an anticancer drug, a safety assessment in dogs showed unexpected retinal toxicity (89). The retina-to-plasma ratio and a low rate of retinal elimination of drugs are reportedly involved in ocular toxicity (90, 91), however, the distribution of the HSP90 inhibitor CH5164840, in the dog was not investigated. A report of a clinical trial of PF-04929113 stated the occurrence of ocular toxicity when the drug was administered daily, but not when it was administered twice a week (84). Whether or not ocular toxicity is observed may reflect differences in exposure to and distribution of the drug. It was considered that clinical trial designs, including administration schedule, might be important for controlling ocular toxicity.

Almost HSP90 inhibitors bind to the ATP pocket in the N-terminal domain of HSP90 and consequently suppress the ATPase activity of HSP90. Recently, some new strategies for HSP90 inhibition have been reported. It was reported that biological activities of HSP90β N-terminal isoform selective inhibitor that are still weak (92). Collectively, it is expected that development of HSP90 inhibitors consists of not only the targeting N-terminal ATP binding site of HSP90, but also of other mechanisms of action.

Acknowledgements

I am deeply grateful to Professor Tomoki Chiba, University of Tsukuba, for overseeing this dissertation, and for valuable discussions throughout my doctoral program; Tetsuo Hashimoto (University of Tsukuba), Yukihiko Tokunaga (Toquenaga) (University of Tsukuba), and Fuminori Tsuruta (University of Tsukuba), for their appropriate advice during the preparation of this dissertation.

I thank Neal Rosen (Memorial Sloan-Kettering Cancer Center), Shigehisa Nagahashi, Hiroshi Sakamoto, Toshiyuki Mio, Osamu Kondo, Atsushi Suda, Takuo Tsukuda, and Yuko Aoki for their helpful discussion; Fumie Sawamura, Yasue Nagata, Sachiya Yamamoto, Yusuke Ide, Ikuko Matsuo, Yumiko Hashimoto, Maiko Izawa, Kurisu Honda, and Kim ByoungJin for their technical support; my coworkers at the Research Division of Chugai Pharmaceutical Co., Ltd. for their encouragement during the project promotion and dissertation preparation.

I gratefully acknowledge Yoshihiko Maehara, Eiji Oki, and Hiroshi Saeki, Department of Surgery and Science, Graduate School of Medical Sciences, Kyushu University, for their helpful discussions and support during the dispatch period at Kyushu University.

Finally, I would like to appreciate my family for support during my time at the University of Tsukuba.

References

1. Whitesell L & Lindquist SL (2005) HSP90 and the chaperoning of cancer. *Nature reviews. Cancer* 5(10):761-772.
2. da Rocha Dias S, *et al.* (2005) Activated B-RAF is an Hsp90 client protein that is targeted by the anticancer drug 17-allylamino-17-demethoxygeldanamycin. *Cancer research* 65(23):10686-10691.
3. Grbovic OM, *et al.* (2006) V600E B-Raf requires the Hsp90 chaperone for stability and is degraded in response to Hsp90 inhibitors. *Proceedings of the National Academy of Sciences of the United States of America* 103(1):57-62.
4. Shimamura T, Lowell AM, Engelman JA, & Shapiro GI (2005) Epidermal growth factor receptors harboring kinase domain mutations associate with the heat shock protein 90 chaperone and are destabilized following exposure to geldanamycins. *Cancer research* 65(14):6401-6408.
5. Bonvini P, Gastaldi T, Falini B, & Rosolen A (2002) Nucleophosmin-anaplastic lymphoma kinase (NPM-ALK), a novel Hsp90-client tyrosine kinase: down-regulation of NPM-ALK expression and tyrosine phosphorylation in ALK(+) CD30(+) lymphoma cells by the Hsp90 antagonist 17-allylamino,17-demethoxygeldanamycin. *Cancer research* 62(5):1559-1566.
6. An WG, Schulte TW, & Neckers LM (2000) The heat shock protein 90 antagonist geldanamycin alters chaperone association with p210bcr-abl and v-src proteins before their degradation by the proteasome. *Cell growth & differentiation : the molecular biology journal of the American Association for Cancer Research* 11(7):355-360.
7. Siegel PM, Ryan ED, Cardiff RD, & Muller WJ (1999) Elevated expression of activated forms of Neu/ErbB-2 and ErbB-3 are involved in the induction of mammary tumors in transgenic mice: implications for human breast cancer. *The EMBO journal* 18(8):2149-2164.
8. Lee-Hoeflich ST, *et al.* (2008) A central role for HER3 in HER2-amplified breast cancer: implications for targeted therapy. *Cancer research* 68(14):5878-5887.
9. Kamal A, *et al.* (2003) A high-affinity conformation of Hsp90 confers tumour selectivity on Hsp90 inhibitors. *Nature* 425(6956):407-410.
10. Pick E, *et al.* (2007) High HSP90 expression is associated with decreased survival in breast cancer. *Cancer research* 67(7):2932-2937.
11. Workman P, Burrows F, Neckers L, & Rosen N (2007) Drugging the cancer chaperone HSP90: combinatorial therapeutic exploitation of oncogene addiction and tumor stress. *Annals of the New York Academy of Sciences* 1113:202-216.
12. Banerji U (2009) Heat shock protein 90 as a drug target: some like it hot. *Clinical cancer research : an official journal of the American Association for Cancer Research* 15(1):9-14.
13. Isaacs JS, Xu W, & Neckers L (2003) Heat shock protein 90 as a molecular target for cancer therapeutics. *Cancer cell* 3(3):213-217.

14. Trepel J, Mollapour M, Giaccone G, & Neckers L (2010) Targeting the dynamic HSP90 complex in cancer. *Nature reviews. Cancer* 10(8):537-549.
15. Yarden Y & Sliwkowski MX (2001) Untangling the ErbB signalling network. *Nature reviews. Molecular cell biology* 2(2):127-137.
16. Bray F, *et al.* (2018) Global cancer statistics 2018: GLOBOCAN estimates of incidence and mortality worldwide for 36 cancers in 185 countries. *CA: a cancer journal for clinicians* 68(6):394-424.
17. Curigliano G, *et al.* (2019) De-escalating and escalating treatments for early-stage breast cancer: the St. Gallen International Expert Consensus Conference on the Primary Therapy of Early Breast Cancer 2017. *Annals of oncology : official journal of the European Society for Medical Oncology* 30(7):1181.
18. Slamon DJ, *et al.* (1987) Human breast cancer: correlation of relapse and survival with amplification of the HER-2/neu oncogene. *Science* 235(4785):177-182.
19. Jaehne J, *et al.* (1992) Expression of Her2/neu oncogene product p185 in correlation to clinicopathological and prognostic factors of gastric carcinoma. *Journal of cancer research and clinical oncology* 118(6):474-479.
20. Campone M, Juin P, Andre F, & Bachelot T (2011) Resistance to HER2 inhibitors: is addition better than substitution? Rationale for the hypothetical concept of drug sedimentation. *Critical reviews in oncology/hematology* 78(3):195-205.
21. Baselga J & Swain SM (2009) Novel anticancer targets: revisiting ERBB2 and discovering ERBB3. *Nature reviews. Cancer* 9(7):463-475.
22. Siegel RL, Miller KD, & Jemal A (2018) Cancer statistics, 2018. *CA: a cancer journal for clinicians* 68(1):7-30.
23. Molina JR, Yang P, Cassivi SD, Schild SE, & Adjei AA (2008) Non-small cell lung cancer: epidemiology, risk factors, treatment, and survivorship. *Mayo Clinic proceedings* 83(5):584-594.
24. Sher T, Dy GK, & Adjei AA (2008) Small cell lung cancer. *Mayo Clinic proceedings* 83(3):355-367.
25. Thompson K & McDougall R (2015) Restricting Access to ART on the Basis of Criminal Record : An Ethical Analysis of a State-Enforced "Presumption Against Treatment" With Regard to Assisted Reproductive Technologies. *Journal of bioethical inquiry* 12(3):511-520.
26. Mitsudomi T, *et al.* (2010) Gefitinib versus cisplatin plus docetaxel in patients with non-small-cell lung cancer harbouring mutations of the epidermal growth factor receptor (WJTOG3405): an open label, randomised phase 3 trial. *The Lancet. Oncology* 11(2):121-128.
27. Zhou C, *et al.* (2011) Erlotinib versus chemotherapy as first-line treatment for patients with advanced EGFR mutation-positive non-small-cell lung cancer (OPTIMAL, CTONG-0802): a multicentre, open-label, randomised, phase 3 study. *The Lancet. Oncology* 12(8):735-742.

28. Taldone T, Gozman A, Maharaj R, & Chiosis G (2008) Targeting Hsp90: small-molecule inhibitors and their clinical development. *Current opinion in pharmacology* 8(4):370-374.
29. Kim YS, *et al.* (2009) Update on Hsp90 inhibitors in clinical trial. *Current topics in medicinal chemistry* 9(15):1479-1492.
30. Porter JR, Fritz CC, & Depew KM (2010) Discovery and development of Hsp90 inhibitors: a promising pathway for cancer therapy. *Current opinion in chemical biology* 14(3):412-420.
31. Xiao Y & Liu Y (2019) Recent Advances in the Discovery of Novel HSP90 Inhibitors: An Update from 2014. *Current drug targets.*
32. Miura T, *et al.* (2011) Lead generation of heat shock protein 90 inhibitors by a combination of fragment-based approach, virtual screening, and structure-based drug design. *Bioorganic & medicinal chemistry letters* 21(19):5778-5783.
33. Suda A, *et al.* (2012) Design and synthesis of novel macrocyclic 2-amino-6-arylpyrimidine Hsp90 inhibitors. *Bioorganic & medicinal chemistry letters* 22(2):1136-1141.
34. Graus-Porta D, Beerli RR, Daly JM, & Hynes NE (1997) ErbB-2, the preferred heterodimerization partner of all ErbB receptors, is a mediator of lateral signaling. *The EMBO journal* 16(7):1647-1655.
35. Holbro T, *et al.* (2003) The ErbB2/ErbB3 heterodimer functions as an oncogenic unit: ErbB2 requires ErbB3 to drive breast tumor cell proliferation. *Proceedings of the National Academy of Sciences of the United States of America* 100(15):8933-8938.
36. Munster PN, Marchion DC, Basso AD, & Rosen N (2002) Degradation of HER2 by ansamycins induces growth arrest and apoptosis in cells with HER2 overexpression via a HER3, phosphatidylinositol 3'-kinase-AKT-dependent pathway. *Cancer research* 62(11):3132-3137.
37. Xu W, *et al.* (2005) Surface charge and hydrophobicity determine ErbB2 binding to the Hsp90 chaperone complex. *Nature structural & molecular biology* 12(2):120-126.
38. Mimnaugh EG, Chavany C, & Neckers L (1996) Polyubiquitination and proteasomal degradation of the p185c-erbB-2 receptor protein-tyrosine kinase induced by geldanamycin. *The Journal of biological chemistry* 271(37):22796-22801.
39. Raja SM, *et al.* (2008) A combination of Trastuzumab and 17-AAG induces enhanced ubiquitinylation and lysosomal pathway-dependent ErbB2 degradation and cytotoxicity in ErbB2-overexpressing breast cancer cells. *Cancer biology & therapy* 7(10):1630-1640.
40. Modi S, *et al.* (2007) Combination of trastuzumab and tanespimycin (17-AAG, KOS-953) is safe and active in trastuzumab-refractory HER-2 overexpressing breast cancer: a phase I dose-escalation study. *Journal of clinical oncology : official journal of the American Society of Clinical Oncology* 25(34):5410-5417.
41. Amin DN, *et al.* (2010) Resiliency and vulnerability in the HER2-HER3 tumorigenic driver. *Science translational medicine* 2(16):16ra17.

42. Sergina NV, *et al.* (2007) Escape from HER-family tyrosine kinase inhibitor therapy by the kinase-inactive HER3. *Nature* 445(7126):437-441.
43. Chandarlapaty S, *et al.* (2011) AKT inhibition relieves feedback suppression of receptor tyrosine kinase expression and activity. *Cancer cell* 19(1):58-71.
44. Lynch TJ, *et al.* (2004) Activating mutations in the epidermal growth factor receptor underlying responsiveness of non-small-cell lung cancer to gefitinib. *The New England journal of medicine* 350(21):2129-2139.
45. Paez JG, *et al.* (2004) EGFR mutations in lung cancer: correlation with clinical response to gefitinib therapy. *Science* 304(5676):1497-1500.
46. Pao W, *et al.* (2004) EGF receptor gene mutations are common in lung cancers from "never smokers" and are associated with sensitivity of tumors to gefitinib and erlotinib. *Proceedings of the National Academy of Sciences of the United States of America* 101(36):13306-13311.
47. Costa DB, Kobayashi S, Tenen DG, & Huberman MS (2007) Pooled analysis of the prospective trials of gefitinib monotherapy for EGFR-mutant non-small cell lung cancers. *Lung cancer* 58(1):95-103.
48. Sharma SV, Bell DW, Settleman J, & Haber DA (2007) Epidermal growth factor receptor mutations in lung cancer. *Nature reviews. Cancer* 7(3):169-181.
49. Engelman JA, *et al.* (2007) MET amplification leads to gefitinib resistance in lung cancer by activating ERBB3 signaling. *Science* 316(5827):1039-1043.
50. Yano S, *et al.* (2008) Hepatocyte growth factor induces gefitinib resistance of lung adenocarcinoma with epidermal growth factor receptor-activating mutations. *Cancer research* 68(22):9479-9487.
51. Sos ML, *et al.* (2009) PTEN loss contributes to erlotinib resistance in EGFR-mutant lung cancer by activation of Akt and EGFR. *Cancer research* 69(8):3256-3261.
52. Pao W, *et al.* (2005) KRAS mutations and primary resistance of lung adenocarcinomas to gefitinib or erlotinib. *PLoS medicine* 2(1):e17.
53. Shaw AT, *et al.* (2009) Clinical features and outcome of patients with non-small-cell lung cancer who harbor EML4-ALK. *Journal of clinical oncology : official journal of the American Society of Clinical Oncology* 27(26):4247-4253.
54. Sequist LV, *et al.* (2011) Genotypic and histological evolution of lung cancers acquiring resistance to EGFR inhibitors. *Science translational medicine* 3(75):75ra26.
55. Kobayashi S, *et al.* (2005) EGFR mutation and resistance of non-small-cell lung cancer to gefitinib. *The New England journal of medicine* 352(8):786-792.
56. Pao W, *et al.* (2005) Acquired resistance of lung adenocarcinomas to gefitinib or erlotinib is associated with a second mutation in the EGFR kinase domain. *PLoS medicine* 2(3):e73.
57. Balak MN, *et al.* (2006) Novel D761Y and common secondary T790M mutations in epidermal

growth factor receptor-mutant lung adenocarcinomas with acquired resistance to kinase inhibitors. *Clinical cancer research : an official journal of the American Association for Cancer Research* 12(21):6494-6501.

58. Sato N, *et al.* (2003) Involvement of heat-shock protein 90 in the interleukin-6-mediated signaling pathway through STAT3. *Biochemical and biophysical research communications* 300(4):847-852.
59. Bromberg JF, *et al.* (1999) Stat3 as an oncogene. *Cell* 98(3):295-303.
60. Gao SP, *et al.* (2007) Mutations in the EGFR kinase domain mediate STAT3 activation via IL-6 production in human lung adenocarcinomas. *The Journal of clinical investigation* 117(12):3846-3856.
61. Mukohara T, *et al.* (2003) Expression of epidermal growth factor receptor (EGFR) and downstream-activated peptides in surgically excised non-small-cell lung cancer (NSCLC). *Lung cancer* 41(2):123-130.
62. Haura EB, Zheng Z, Song L, Cantor A, & Bepler G (2005) Activated epidermal growth factor receptor-Stat-3 signaling promotes tumor survival in vivo in non-small cell lung cancer. *Clinical cancer research : an official journal of the American Association for Cancer Research* 11(23):8288-8294.
63. Ono N, *et al.* (2012) Preclinical antitumor activity of the novel heat shock protein 90 inhibitor CH5164840 against human epidermal growth factor receptor 2 (HER2)-overexpressing cancers. *Cancer science* 103(2):342-349.
64. Song L, Rawal B, Nemeth JA, & Haura EB (2011) JAK1 activates STAT3 activity in non-small-cell lung cancer cells and IL-6 neutralizing antibodies can suppress JAK1-STAT3 signaling. *Molecular cancer therapeutics* 10(3):481-494.
65. Hirsch FR, *et al.* (2007) Combination of EGFR gene copy number and protein expression predicts outcome for advanced non-small-cell lung cancer patients treated with gefitinib. *Annals of oncology : official journal of the European Society for Medical Oncology* 18(4):752-760.
66. Pao W & Chmielecki J (2010) Rational, biologically based treatment of EGFR-mutant non-small-cell lung cancer. *Nature reviews. Cancer* 10(11):760-774.
67. Ogino A, *et al.* (2007) Emergence of epidermal growth factor receptor T790M mutation during chronic exposure to gefitinib in a non small cell lung cancer cell line. *Cancer research* 67(16):7807-7814.
68. Yamamoto C, *et al.* (2010) Loss of PTEN expression by blocking nuclear translocation of EGR1 in gefitinib-resistant lung cancer cells harboring epidermal growth factor receptor-activating mutations. *Cancer research* 70(21):8715-8725.
69. Zhang Z, *et al.* (2012) Activation of the AXL kinase causes resistance to EGFR-targeted therapy in lung cancer. *Nature genetics* 44(8):852-860.
70. Shimamura T, *et al.* (2008) Hsp90 inhibition suppresses mutant EGFR-T790M signaling and

overcomes kinase inhibitor resistance. *Cancer research* 68(14):5827-5838.

71. Koizumi H, *et al.* (2012) Hsp90 inhibition overcomes HGF-triggering resistance to EGFR-TKIs in EGFR-mutant lung cancer by decreasing client protein expression and angiogenesis. *Journal of thoracic oncology : official publication of the International Association for the Study of Lung Cancer* 7(7):1078-1085.
72. Sequist LV, *et al.* (2010) Activity of IPI-504, a novel heat-shock protein 90 inhibitor, in patients with molecularly defined non-small-cell lung cancer. *Journal of clinical oncology : official journal of the American Society of Clinical Oncology* 28(33):4953-4960.
73. Guo F, *et al.* (2005) Abrogation of heat shock protein 70 induction as a strategy to increase antileukemia activity of heat shock protein 90 inhibitor 17-allylamino-demethoxy geldanamycin. *Cancer research* 65(22):10536-10544.
74. Powers MV, *et al.* (2010) Targeting HSP70: the second potentially druggable heat shock protein and molecular chaperone? *Cell cycle* 9(8):1542-1550.
75. Tsao MS, *et al.* (2005) Erlotinib in lung cancer - molecular and clinical predictors of outcome. *The New England journal of medicine* 353(2):133-144.
76. Hirsch FR, *et al.* (2006) Molecular predictors of outcome with gefitinib in a phase III placebo-controlled study in advanced non-small-cell lung cancer. *Journal of clinical oncology : official journal of the American Society of Clinical Oncology* 24(31):5034-5042.
77. Rice JW, *et al.* (2009) Targeting of multiple signaling pathways by the Hsp90 inhibitor SNX-2112 in EGFR resistance models as a single agent or in combination with erlotinib. *Oncology research* 18(5-6):229-242.
78. Bao R, *et al.* (2009) Targeting heat shock protein 90 with CUDC-305 overcomes erlotinib resistance in non-small cell lung cancer. *Molecular cancer therapeutics* 8(12):3296-3306.
79. Solca F, *et al.* (2012) Target binding properties and cellular activity of afatinib (BIBW 2992), an irreversible ErbB family blocker. *The Journal of pharmacology and experimental therapeutics* 343(2):342-350.
80. Cross DA, *et al.* (2014) AZD9291, an irreversible EGFR TKI, overcomes T790M-mediated resistance to EGFR inhibitors in lung cancer. *Cancer discovery* 4(9):1046-1061.
81. Mok TS, *et al.* (2017) Osimertinib or Platinum-Pemetrexed in EGFR T790M-Positive Lung Cancer. *The New England journal of medicine* 376(7):629-640.
82. Messaoudi S, Peyrat JF, Brion JD, & Alami M (2011) Heat-shock protein 90 inhibitors as antitumor agents: a survey of the literature from 2005 to 2010. *Expert opinion on therapeutic patents* 21(10):1501-1542.
83. Kummar S, *et al.* (2010) Phase I trial of 17-dimethylaminoethylamino-17-demethoxygeldanamycin (17-DMAG), a heat shock protein inhibitor, administered twice weekly in patients with advanced malignancies. *Eur. J. Cancer* 46(2):340-347.

84. Rajan A, *et al.* (2011) A phase I study of PF-04929113 (SNX-5422), an orally bioavailable heat shock protein 90 inhibitor, in patients with refractory solid tumor malignancies and lymphomas. *Clinical cancer research : an official journal of the American Association for Cancer Research* 17(21):6831-6839.

85. T. A. Samuel CS, C. Britten, K. S. Milligan, M. M. Mita, U. Banerji, T. J. Pluard, P. Stiegler, C. Quadt and G. Shapiro (2010) AUY922, a novel HSP90 inhibitor: Final results of a first-in-human study in patients with advanced solid malignancies. *J. Clin. Oncol.* 28(15s):suppl; abstr 2528.

86. G. Shapiro ELK, B. J. Dezube, D. P. Lawrence, J. M. Cleary, S. Lewis, M. Squires, V. Lock, J. F. Lyons, and M. Yule (2010) Phase I pharmacokinetic and pharmacodynamic study of the heat shock protein 90 inhibitor AT13387 in patients with refractory solid tumors. *J. Clin. Oncol.* 28:suppl; abstr 3069.

87. Solit DB, *et al.* (2007) Phase I trial of 17-allylamino-17-demethoxygeldanamycin in patients with advanced cancer. *Clin. Cancer Res.* 13(6):1775-1782.

88. Socinski MA, *et al.* (2013) A multicenter phase II study of ganetespib monotherapy in patients with genotypically defined advanced non-small cell lung cancer. *Clin. Cancer Res.* 19(11):3068-3077.

89. Kanamaru C, *et al.* (2014) Retinal toxicity induced by small-molecule Hsp90 inhibitors in beagle dogs. *The Journal of toxicological sciences* 39(1):59-69.

90. Zhou D, *et al.* (2013) A rat retinal damage model predicts for potential clinical visual disturbances induced by Hsp90 inhibitors. *Toxicol. Appl. Pharmacol.* 273(2):401-409.

91. Ohkubo S, *et al.* (2015) TAS-116, a highly selective inhibitor of heat shock protein 90alpha and beta, demonstrates potent antitumor activity and minimal ocular toxicity in preclinical models. *Molecular cancer therapeutics* 14(1):14-22.

92. Khandelwal A, *et al.* (2018) Structure-guided design of an Hsp90beta N-terminal isoform-selective inhibitor. *Nature communications* 9(1):425.

List of Publications

1. Ono N, Yamazaki T, Nakanishi Y, Fujii T, SakatAKTachibana Y, Suda A, Hada K, Miura T, Sato S, Saitoh R, Nakano K, Tsukuda T, Mio T, Ishii N, Kondoh O, Aoki Y.
Preclinical antitumor activity of the novel heat shock protein 90 inhibitor CH5164840 against human epidermal growth factor receptor 2 (HER2)-overexpressing cancers.
Cancer Science. 2012 Feb;103(2):342-349.

2. Ono N, Yamazaki T, Tsukaguchi T, Fujii T, Sakata K, Suda A, Tsukuda T, Mio T, Ishii N, Kondoh O, Aoki Y.
Enhanced antitumor activity of erlotinib in combination with the HSP90 inhibitor CH5164840 against non-small-cell lung cancer.
Cancer Science. 2013 Oct;104(10):1346-1352